

Robust and Computationally Efficient Trimmed L -Moments Estimation for Parametric Distributions

CHUDAMANI POUDYAL¹ 

University of Central Florida

QIAN ZHAO² 

Robert Morris University

HARI SITAULA³

Montana Technological University

© Copyright of this Manuscript is held by the Authors!

Abstract. This paper proposes a robust and computationally efficient estimation framework for fitting parametric distributions based on trimmed L -moments. Trimmed L -moments extend classical L -moment theory by downweighting or excluding extreme order statistics, resulting in estimators that are less sensitive to outliers and heavy tails. We construct estimators for both location-scale and shape parameters using asymmetric trimming schemes tailored to different moments, and establish their asymptotic properties for inferential justification using the general structural theory of L -statistics, deriving simplified single-integration expressions to ensure numerical stability. State-of-the-art algorithms are developed to resolve the sign ambiguity in estimating the scale parameter for location-scale models and the tail index for the Fréchet model. The proposed estimators offer improved efficiency over traditional robust alternatives for selected asymmetric trimming configurations, while retaining closed-form expressions for a wide range of common distributions, facilitating fast and stable computation. Simulation studies demonstrate strong finite-sample performance. An application to financial claim severity modeling highlights the practical relevance and flexibility of the approach.

Keywords. Computational efficiency; Location-scale models; L -statistics; Robust estimation; Tail index estimation; Trimmed L -moments.

¹CORRESPONDING AUTHOR: Chudamani Poudyal, PhD, ASA, is an Assistant Professor in the Department of Statistics and Data Science, University of Central Florida, Orlando, FL 32816, USA. *e-mail:* Chudamani.Poudyal@ucf.edu

²Qian Zhao, PhD, ASA, is an Associate Professor in the Department of Mathematics, Robert Morris University, Moon Township, PA 15108, USA. *e-mail:* zhao@rmu.edu

³Hari Sitaula, PhD, is an Assistant Professor in the Department of Mathematical Sciences, Montana Technological University, Butte, MT 59701, USA. *e-mail:* Hsitaula@mtech.edu

1 Introduction

Robust and computationally efficient parameter estimation is essential in statistical learning, especially under data contamination, measurement error, or heavy tails. While the maximum likelihood estimator (MLE) is asymptotically efficient under correct model assumptions, it is well known to be highly sensitive to deviations from ideal conditions and to contamination in the data (Hampel *et al.*, 1986, Huber and Ronchetti, 2009). These issues frequently arise in real-world settings such as biomedical studies, engineering reliability analysis, and environmental monitoring, where irregularities and extreme values are often present. Robust statistics provides a formal framework for addressing such challenges by developing estimators that maintain good performance even when standard assumptions are violated. These procedures aim to reduce the influence of atypical data while preserving efficiency, ensuring stability and interpretability in practical applications.

The theory of robust statistics has been systematically developed since the mid-1960s (Tukey, 1960), with foundational work introducing methods to reduce the sensitivity of estimators to model misspecification and data contamination (Huber and Ronchetti, 2009). Within this framework, the method of trimmed moments (MTM)—a subclass of L -moments (Chernoff *et al.*, 1967)—has gained attention as a practical and computationally efficient alternative to likelihood-based estimation. MTM replaces classical moments with trimmed moments computed by excluding extreme order statistics, yielding estimators that are finite, stable, and robust to outliers. These estimators have been developed for various distributional families, including location-scale models, exponential-type distributions, and heavy-tailed models (Brazauskas *et al.*, 2009, Brazauskas and Kleefeld, 2009, Kleefeld and Brazauskas, 2012). MTMs have also been applied in several domains: Opdyke and Cavallo (2012) used them in operational risk modeling, Kim and Jeon (2013) applied them in credibility theory, and Hao *et al.* (2014) used them to construct bootstrap confidence intervals for reliability data. Their application to incomplete loss data has been further examined by Poudyal (2021) and Poudyal and Brazauskas (2023), demonstrating that MTM provides an effective framework for enhancing robustness by mitigating the influence of heavy point masses at left truncation and right censoring boundaries (Gatti and Wüthrich, 2025).

Despite the existence of general asymptotic distributional results for MTM, independently established by Chernoff *et al.* (1967) and Brazauskas *et al.* (2009), and their equivalence formally shown by Poudyal (2025), most existing implementations adopt a single trimming configuration uniformly across all moments, regardless of the number of parameters to be estimated or the distributional

features of the data. This constraint can lead to different or suboptimal subsets of data being used for estimating each moment, reducing efficiency or discarding relevant information. To address this limitation, [Poudyal \(2025\)](#) developed computationally tractable expressions for the asymptotic distribution of MTM estimators that allow for distinct trimming proportions for each moment. This extension maintains the foundational asymptotic structure of L -statistics ([Chernoff *et al.*, 1967](#)) while allowing practitioners to achieve a more effective robustness-efficiency trade-off tailored to the nature of the parameter being estimated.

Therefore, this work introduces a general and flexible framework for robust estimation using trimmed L -moments that allows for *distinct trimming proportions across different moments*.

This framework tailors trimming to moment-specific sensitivity, accommodating asymmetry where needed and enabling a more effective balance between robustness and efficiency. The proposed framework includes previously studied symmetric-trimming methods as special cases, while extending the modeling flexibility to better adapt to real-world data structures. We develop closed-form estimators and their asymptotic distributional properties for location-scale and Fréchet models under the general L -statistic framework, along with computational expressions for analytic variance. The estimators do not require iterative optimization, making them computationally efficient and scalable to large datasets. The explicit nature of the estimators ensures numerical stability and reproducibility—key requirements for scalable statistical methods in scientific computing and industrial analytics. We also address the sign ambiguity in scale and shape estimation through a principled selection strategy based on proximity to the full-sample estimate. The proposed methods are validated through extensive simulation studies and real-data applications, confirming their strong finite-sample performance and practical relevance.

The remainder of the paper is organized as follows. Section 2 introduces the general L -estimator framework and derives its theoretical properties, specifically focusing on MTM. Section 3 is the section where we implement the designed methodology for specific parcomprehensive simulation study, and Section 5 provides real-data applications. Section 6 concludes with a discussion and future directions.

2 General Method of Trimmed L -Moments

Consider a random variable X with the cdf $F(x|\boldsymbol{\theta})$, where $\boldsymbol{\theta} = (\theta_1, \dots, \theta_k)$, for some positive integer k , is the parameter vector to be estimated. Consider a random sample X_1, \dots, X_n of size n with the corresponding order statistics $X_{1:n} \leq \dots \leq X_{n:n}$. Then the *method of trimmed moments* (MTM) estimators of $\theta_1, \theta_2, \dots, \theta_k$ are found as follows:

- Compute the sample trimmed moments

$$\widehat{T}_j = \frac{1}{n - \lfloor na_j \rfloor - \lfloor nb_j \rfloor} \sum_{i=\lfloor na_j \rfloor + 1}^{n - \lfloor nb_j \rfloor} h_j(X_{i:n}), \quad 1 \leq j \leq k. \quad (1)$$

The h'_j s in (1) are specially chosen functions for mathematical convenience and are typically specified by the data analyst. For a detailed discussion, we refer the reader to [Brazauskas et al. \(2009\)](#) and [Poudyal \(2021\)](#). The proportions $0 \leq a_j, b_j \leq 1$ should be selected based on the desired balance between efficiency and robustness.

- Compute the corresponding population trimmed moments

$$T_j = \frac{1}{1 - a_j - b_j} \int_{a_j}^{\bar{b}_j} H_j(u) du, \quad 1 \leq j \leq k, \quad \bar{v} := 1 - v, \quad v \in [0, 1]. \quad (2)$$

In (2), $F^{-1}(u|\boldsymbol{\theta}) = \inf \{x : F(x|\boldsymbol{\theta}) \geq u\}$ is the quantile function, and $H_j := h_j \circ F^{-1}$.

- Match the sample and population trimmed moments from (1) and (2) to get the following system of equations for $\theta_1, \theta_2, \dots, \theta_k$:

$$\begin{cases} T_1(\theta_1, \dots, \theta_k) &= \widehat{T}_1, \\ &\vdots \\ T_k(\theta_1, \dots, \theta_k) &= \widehat{T}_k. \end{cases} \quad (3)$$

A solution, say $\widehat{\boldsymbol{\theta}}_T = (\widehat{\theta}_1, \widehat{\theta}_2, \dots, \widehat{\theta}_k)$, if it exists, to the system of equations (3) is called the *method of trimmed moments (MTM)* estimator of $\boldsymbol{\theta}$. Thus, $\widehat{\theta}_j =: g_j(\widehat{T}_1, \widehat{T}_2, \dots, \widehat{T}_k)$, $1 \leq j \leq k$, are the MTM estimators of $\theta_1, \theta_2, \dots, \theta_k$.

Asymptotically, Eq. (1) is equivalent to a general structure of L -statistics under the condition $0 \leq a_j < \bar{b}_j \leq 1$ with $a_j + b_j < 1$; see [Serfling \(1980, p. 264\)](#). Specifically,

$$\widehat{T}_j := \frac{1}{n} \sum_{i=1}^n J_j \left(\frac{i}{n+1} \right) h_j(X_{i:n}), \quad 1 \leq j \leq k, \quad (4)$$

with the specified weights-generating function:

$$J_j(s) = \begin{cases} (1 - a_j - b_j)^{-1}; & a_j < s < \bar{b}_j, \\ 0; & \text{otherwise.} \end{cases} \quad 1 \leq j \leq k, \quad (5)$$

Similarly, Eq. (2) is equivalent to

$$T_j \equiv T_j(\boldsymbol{\theta}) \equiv T_j(\theta_1, \dots, \theta_k) = \int_0^1 J_j(u) H_j(u) du. \quad (6)$$

We define

$$\hat{\mathbf{T}} := (\hat{T}_1, \hat{T}_1, \dots, \hat{T}_k) \quad \text{and} \quad \mathbf{T} := (T_1, T_2, \dots, T_k). \quad (7)$$

As sample statistics, the vector $\hat{\mathbf{T}}$ is expected to converge in distribution to the corresponding population parameter \mathbf{T} . In total, there are six possible combinations of trimming proportions (a_i, b_i) and (a_j, b_j) for $1 \leq i, j \leq k$; see [Poudyal \(2025\)](#) for a detailed discussion. Among these, we focus on the case defined by the following inequality:

$$0 \leq a_j \leq a_i < \bar{b}_j \leq \bar{b}_i \leq 1. \quad (8)$$

Under the trimming inequality (8), and following the general asymptotic distributional results of [Chernoff et al. \(1967\)](#), the asymptotic distribution of the vector $\hat{\mathbf{T}}$, along with the computational expressions developed by [Poudyal \(2025\)](#), is summarized in Theorem 1. The result is based on the following two integral quantities and a kernel function.

Following [Poudyal \(2025\)](#), for $1 \leq i \leq k$ and $0 \leq a \leq b \leq 1$, define

$$\begin{cases} I_i(a, b) := b H_i(b) - a H_i(a) - \int_a^b H_i(v) dv, \\ \bar{I}_i(a, b) := \bar{b} H_i(b) - \bar{a} H_i(a) + \int_a^b H_i(v) dv, \end{cases} \quad (9)$$

and define the kernel function $K(w, v)$ as

$$K(w, v) := K(v, w) = \min\{w, v\} - wv, \quad \text{for } 0 \leq w, v \leq 1. \quad (10)$$

Theorem 1. *With the trimming proportions satisfying inequality (8), it follows that*

$$\sqrt{n} (\hat{\mathbf{T}} - \mathbf{T}) \sim \mathcal{AN}(\mathbf{0}, \boldsymbol{\Sigma}_T), \quad \boldsymbol{\Sigma}_T = [\sigma_{ij}^2]_{i,j=1}^k, \quad \sigma_{ij}^2 = \Gamma(i, j) V(i, j), \quad (11)$$

where

$$\Gamma \equiv \Gamma(i, j) = \prod_{r=i,j} (1 - a_r - b_r)^{-1}, \quad (12)$$

$$V(i, j) = \int_{a_i}^{\bar{b}_i} \int_{a_j}^{\bar{b}_j} K(v, w) H'_j(v) H'_i(w) dv dw \quad (13)$$

$$\begin{aligned} &= I_j(a_j, a_i) \bar{I}_i(a_i, \bar{b}_i) + b_i H_i(\bar{b}_i) I_j(a_i, \bar{b}_j) - a_i H_i(a_i) \bar{I}_j(a_i, \bar{b}_j) + \int_{a_i}^{\bar{b}_j} H_i(v) H_j(v) dv \\ &\quad + [\bar{b}_j H_j(\bar{b}_j) - a_i H_j(a_i)] \int_{\bar{b}_j}^{\bar{b}_i} H_i(v) dv - [a_i H_j(a_i) + b_j H_j(\bar{b}_j)] \int_{a_i}^{\bar{b}_j} H_i(v) dv \\ &\quad - \left(\int_{a_i}^{\bar{b}_j} H_j(v) dv \right) \left(\int_{a_i}^{\bar{b}_j} H_i(v) dv \right) - \left(\int_{a_i}^{\bar{b}_j} H_j(v) dv \right) \left(\int_{\bar{b}_j}^{\bar{b}_i} H_i(v) dv \right). \end{aligned} \quad (14)$$

Different trimming proportions for different moments were used by [Brazauskas and Kleefeld \(2009\)](#) to estimate the parameters of generalized Pareto distributions. While they approximated the entries σ_{ij}^2 of the variance-covariance matrix Σ_T directly from Eq. (13) using a numerical bivariate trapezoidal rule ([Brazauskas and Kleefeld, 2009, Appendix A.2](#)), our approach derives the simplified closed-form expression in Eq. (14), as presented in Theorem 1.

Note 1. If the trimming inequality (8) is replaced by

$$0 \leq a_i \leq a_j < \bar{b}_i \leq \bar{b}_j \leq 1, \quad (15)$$

then the asymptotic result in Theorem 1 remains still valid by simply interchanging the indices i and j . \square

Using the delta method (see, e.g., [Serfling, 1980, Theorem A, p. 122](#)), along with $\hat{\mathbf{T}} = (\hat{T}_1, \dots, \hat{T}_k)$ and $\theta_j = g_j(T_1(\boldsymbol{\theta}), \dots, T_k(\boldsymbol{\theta}))$, we present the following asymptotic result for $\hat{\boldsymbol{\theta}}_T$.

Theorem 2 (Delta method). *The MTM-estimator of $\boldsymbol{\theta}$, denoted by $\hat{\boldsymbol{\theta}}_T$, has the following asymptotic distribution:*

$$\hat{\boldsymbol{\theta}}_T = (\hat{\theta}_1, \dots, \hat{\theta}_k) \sim \mathcal{AN} \left(\boldsymbol{\theta}, \frac{1}{n} \mathbf{S}_T \right), \quad \mathbf{S}_T := \mathbf{D}_T \boldsymbol{\Sigma}_T \mathbf{D}'_T, \quad (16)$$

where the Jacobian \mathbf{D}_T is given by $\mathbf{D}_T = \left[\frac{\partial g_i}{\partial \hat{T}_j} \Big|_{\hat{\mathbf{T}}=\mathbf{T}} \right]_{k \times k} =: [d_{ij}]_{k \times k}$ and the variance-covariance matrix $\boldsymbol{\Sigma}_T$ has the same form as in Theorem 1.

With the asymptotic distributional properties from Theorem 2, the asymptotic performance of MTM-estimators are assessed by computing their asymptotic relative efficiency (ARE) in relation to the maximum likelihood estimator (MLE). For a model parameterized by k parameters, the ARE is defined as (see, e.g., [Serfling, 1980](#)):

$$ARE(\mathcal{C}, \text{MLE}) = \left(\frac{\det(\boldsymbol{\Sigma}_{\text{MLE}})}{\det(\boldsymbol{\Sigma}_c)} \right)^{1/k}, \quad (17)$$

where Σ_{MLE} and Σ_c are the asymptotic covariance matrices of the MLE and the MTM-estimator \mathcal{C} , respectively, with \det denoting the determinant operation on a square matrix. The MLE serves as a reference due to its superior asymptotic efficiency regarding variance, contingent on specific regularity conditions being met. For additional insights, consult [Serfling \(1980\)](#), Section 4.1.

Note 2. *With trimming proportions satisfying $0 \leq a_i \leq \bar{b}_i \leq 1$, if $a_i > 0$, $b_i > 0$, and $a_i + b_i < 1$ for $1 \leq i \leq k$, then the resulting estimators are globally robust with lower and upper breakdown points*

$$LBP = \min\{a_1, a_2, \dots, a_k\} \quad \text{and} \quad UBP = \min\{b_1, b_2, \dots, b_k\}.$$

These breakdown points quantify resistance to outliers: observations with order less than $n \times LBP$ or greater than $n \times (1 - UBP)$ are effectively excluded from the estimation procedure. Such trimming ensures robustness against extreme values on both ends of the distribution. For a rigorous treatment of breakdown points and robust estimation under heavy-tailed models, see [Hampel et al. \(1986\)](#) and [Serfling \(2002\)](#). \square

3 Parametric Examples

In this section, we derive general MTM estimators for the location and scale parameters of broad location-scale families, which are not necessarily symmetric, while also highlighting the advantages of the general MTM framework when the distribution is symmetric about zero. We also obtain the entries of the corresponding asymptotic variance-covariance matrix. For numerical illustrations, we consider the lognormal and Fréchet distributions and present state-of-the-art algorithms designed to resolve the sign ambiguity in estimating the scale parameter for location-scale models and the tail index for the Fréchet model. Additionally, we evaluate the asymptotic relative efficiency (ARE) of the MTM estimators with respect to the maximum likelihood estimator (MLE), as defined in Eq. (17).

3.1 Location Scale Model

Consider $X_1, X_2, \dots, X_n \stackrel{iid}{\sim} X$, where X is a location-scale random variable with the CDF

$$F(x) = F_0\left(\frac{x - \theta}{\sigma}\right), \quad -\infty < x < \infty, \tag{18}$$

where $-\infty < \theta < \infty$ and $\sigma > 0$ are, respectively, the location and scale parameters of X , and F_0 is the standard parameter-free version of F , i.e., with $\theta = 0$ and $\sigma = 1$. The corresponding

percentile/quantile function of X is given by

$$F^{-1}(u) = \theta + \sigma F_0^{-1}(u). \quad (19)$$

Since we are estimating two unknown parameters, θ and σ , we equate the first two sample trimmed-moments with their corresponding population trimmed-moments. Further, knowing $-\infty < \theta < \infty$ and $\sigma > 0$, we choose

$$h_1(x) = x \quad \text{and} \quad h_2(x) = x^2. \quad (20)$$

From Eq. (6), we note that $H_j := h_j \circ F^{-1}$. Then, from Eq. (19) and Eq. (20), we have

$$H_1(u) = h_1(F^{-1}(u)) = F^{-1}(u) = \theta + \sigma F_0^{-1}(u), \quad (21)$$

$$\implies dH_1(u) = \sigma dF_0^{-1}(u), \quad (22)$$

$$H_2(u) = h_2(F^{-1}(u)) = \theta^2 + 2\theta\sigma F_0^{-1}(u) + \sigma^2 [F_0^{-1}(u)]^2, \quad (23)$$

$$\implies dH_2(u) = 2\theta\sigma dF_0^{-1}(u) + 2\sigma^2 F_0^{-1}(u) dF_0^{-1}(u). \quad (24)$$

With only two parameters, θ and σ , to estimate, we focus on the trimming inequality derived from (8), stated explicitly as:

$$0 \leq a_2 \leq a_1 < \bar{b}_2 \leq \bar{b}_1 \leq 1. \quad (25)$$

With the trimming proportions (a_1, b_1) and (a_2, b_2) as given in (25), then from Eq. (1), the first two sample trimmed-moments are given by:

$$\begin{cases} \hat{T}_1 = \frac{1}{n - \lfloor na_1 \rfloor - \lfloor nb_1 \rfloor} \sum_{i=\lfloor na_1 \rfloor + 1}^{n - \lfloor nb_1 \rfloor} h_1(X_{i:n}) = \frac{1}{n - \lfloor na_1 \rfloor - \lfloor nb_1 \rfloor} \sum_{i=\lfloor na_1 \rfloor + 1}^{n - \lfloor nb_1 \rfloor} X_{i:n}, \\ \hat{T}_2 = \frac{1}{n - \lfloor na_2 \rfloor - \lfloor nb_2 \rfloor} \sum_{i=\lfloor na_2 \rfloor + 1}^{n - \lfloor nb_2 \rfloor} h_2(X_{i:n}) = \frac{1}{n - \lfloor na_2 \rfloor - \lfloor nb_2 \rfloor} \sum_{i=\lfloor na_2 \rfloor + 1}^{n - \lfloor nb_2 \rfloor} X_{i:n}^2. \end{cases} \quad (26)$$

The corresponding first two population trimmed-moments using Eq. (2) takes the form:

$$\begin{cases} T_1 \equiv T_1(\theta, \sigma) = \frac{1}{1 - a_1 - b_1} \int_{a_1}^{\bar{b}_1} H_1(u) du = \theta + \sigma c_1(a_1, \bar{b}_1), \\ T_2 \equiv T_2(\theta, \sigma) = \frac{1}{1 - a_2 - b_2} \int_{a_2}^{\bar{b}_2} H_2(u) du = \theta^2 + 2\theta\sigma c_1(a_2, \bar{b}_2) + \sigma^2 c_2(a_2, \bar{b}_2), \end{cases} \quad (27)$$

where

$$c_k(a, b) \equiv c_k(F_0, a, b) = \frac{1}{b-a} \int_a^b [F_0^{-1}(u)]^k du, \quad k \geq 1. \quad (28)$$

Equating $T_1 = \widehat{T}_1$ and $T_2 = \widehat{T}_2$, and solving the resulting system of equations, we obtain the explicit expressions for θ and σ as:

$$\begin{cases} \widehat{\theta}_T = \widehat{T}_1 - c_1(a_1, \bar{b}_1) \widehat{\sigma}_T =: g_1(\widehat{T}_1, \widehat{T}_2), \\ \widehat{\sigma}_T = \frac{\pm 1}{\sqrt{\eta(a_1, \bar{b}_2)}} (\widehat{T}_2 - \eta_r \widehat{T}_1^2)^{1/2} + \frac{\widehat{T}_1 (c_1(a_1, \bar{b}_1) - c_1(a_2, \bar{b}_2))}{\eta(a_1, \bar{b}_2)} =: g_2(\widehat{T}_1, \widehat{T}_2), \end{cases} \quad (29)$$

where for $1 \leq i, j \leq 2$,

$$\eta(a_i, \bar{b}_j) := c_1^2(a_i, \bar{b}_i) - 2c_1(a_i, \bar{b}_i)c_1(a_j, \bar{b}_j) + c_2(a_j, \bar{b}_j), \quad \eta_r := \frac{\eta(a_j, \bar{b}_j)}{\eta(a_i, \bar{b}_j)}. \quad (30)$$

Note 3. The motivation for imposing the trimming inequality (25) is to ensure that the same data points are trimmed from both tails for the first and second moments, particularly when the sample data are approximately symmetric about zero, an approach that, to our knowledge, has not been fully addressed in the existing literature.

For illustration, consider the sample dataset:

$$-15, -13, -8, -4, -2, 3, 5, 7, 9, 12.$$

- Under equal trimming proportions, say $(a_1, b_1) = (a_2, b_2) = (0.2, 0.2)$, the trimmed samples are:

Trimmed sample for the first moment: $-8, -4, -2, 3, 5, 7$.

Trimmed sample for the second moment: $(-4)^2, 5^2, 7^2, (-8)^2, 9^2, 12^2$.

In this case, observations $-15, -13, 9$, and 12 are trimmed for the first moment, whereas $-15, -13, -2$, and 3 are trimmed for the second moment. Hence, different data points are being trimmed for the first and second moments.

- Now consider unequal trimming proportions, e.g., $(a_1, b_1) = (0.2, 0.2)$ and $(a_2, b_2) = (0, 0.4)$, which yield:

Trimmed sample for the first moment: $-8, -4, -2, 3, 5, 7$.

Trimmed sample for the second moment: $(-8)^2, (-4)^2, (-2)^2, 3^2, 5^2, 7^2$.

In this case, the same observations $-15, -13, 9$, and 12 are trimmed from both the first and second moments.

Therefore, if the data arise from a distribution symmetric about zero, ensuring that the same observations are trimmed from both the first and second moments generally requires using different trimming proportions, i.e., $(a_1, b_1) \neq (a_2, b_2)$.

Even when all observations are negative, equal trimming proportions—e.g., $(a_1, b_1) = (a_2, b_2) = (0.1, 0.2)$ —can still result in trimming different observations for the first and second moments. In contrast, if all data points are positive, then equal trimming proportions typically lead to trimming the same observations for both moments.

Nevertheless, to enhance robustness, one may deliberately choose different trimming proportions that result in trimming different observations for the first and second moments—even when the underlying model assumes strictly positive support. In such cases, it is advisable to select trimming parameters that satisfy the condition

$$0 \leq a_1 \leq a_2 < \bar{b}_1 \leq \bar{b}_2 \leq 1, \quad (31)$$

which allows greater flexibility in capturing potential distributional asymmetries and tail behaviors.

Therefore, our motivation for adopting the trimming inequality (25) is to ensure consistent trimming across both moments when the underlying distribution is symmetric about zero, whereas inequality (31) offers an alternative strategy to enhance robustness when the random variable is strictly positive.

□

Proposition 1. With the trimming proportions (a_i, b_i) and (a_j, b_j) satisfying the inequality (8), it follows that

$$(i) \quad \eta(a_i, \bar{b}_j) = c_1^2(a_i, \bar{b}_i) - 2c_1(a_i, \bar{b}_i)c_1(a_j, \bar{b}_j) + c_2(a_j, \bar{b}_j) > 0.$$

$$(ii) \quad c_k(a_i, \bar{b}_i) \geq c_k(a_j, \bar{b}_j), \text{ for any odd positive integer } k.$$

$$(iii) \quad 0 < \eta_r = \frac{\eta(a_j, \bar{b}_j)}{\eta(a_i, \bar{b}_j)} \leq 1.$$

$$(iv) \quad c_2(a_j, \bar{b}_j) \geq \eta_r c_1^2(a_i, \bar{b}_i).$$

$$(v) \quad T_2 - \eta_r T_1^2 \geq 0.$$

Proof. See Appendix A. \square

Note 4. Under the inequality condition (25), no fixed ordering can be established between $c_2(a_2, \bar{b}_2)$ and $c_1^2(a_1, \bar{b}_1)$, or equivalently between T_2 and T_1^2 . To illustrate both possible directions, consider the standard normal distribution, i.e., $F_0 = \Phi$, with $\theta = 0$ and $\sigma = 1$. Then:

1. For $a_2 = 0.02$, $\bar{b}_2 = 0.75$ and $a_1 = 0.05$, $\bar{b}_1 = 0.99$,

$$T_2 = c_2(a_2, \bar{b}_2) = 0.5702 > 0.0066 = c_1^2(a_1, \bar{b}_1) = T_1^2.$$

2. For $a_2 = 0.02$, $\bar{b}_2 = 0.75$ and $a_1 = 0.50$, $\bar{b}_1 = 0.99$,

$$T_2 = c_2(a_2, \bar{b}_2) = 0.5702 < 0.5773 = c_1^2(a_1, \bar{b}_1) = T_1^2.$$

However, by Proposition 1 (iv), the inequality is restored as below

$$c_2(a_2, \bar{b}_2) \geq \eta_r c_1^2(a_1, \bar{b}_1), \quad \text{equivalently} \quad T_2 - \eta_r T_1^2 \geq 0.$$

Similarly, for a nonzero location parameter, say $\theta = 5$ and $\sigma = 2$, we observe that

$$T_2 = 19.9010 \leq T_1^2 = 42.5046, \quad \text{but} \quad T_2 = 19.9010 \geq \eta_r T_1^2 = 10.8001. \quad (32)$$

\square

Corollary 1. Under the trimming inequality (15), that is, (31) for location-scale models, all results of Proposition 1 remain valid except for Part (ii), which instead takes the form $c_k(a_i, \bar{b}_i) \leq c_k(a_j, \bar{b}_j)$, for any odd positive integer k .

Note 5. Define

$$\sigma_{FT} = \frac{1}{\sqrt{\eta(a_1, \bar{b}_2)}} (T_2 - \eta_r T_1^2)^{1/2} \quad \text{and} \quad \sigma_{ST} = \frac{T_1 (c_1(a_1, \bar{b}_1) - c_1(a_2, \bar{b}_2))}{\eta(a_1, \bar{b}_2)}. \quad (33)$$

Under the trimming inequality (25), a consistent directional relationship between σ_{FT} and σ_{ST} is not guaranteed.

For illustration, consider $X \sim N(\theta = 10, \sigma = 3)$. Then, for

$$(a_1, b_1) = (0.02, 0.02) \quad \text{and} \quad (a_2, b_2) = (0.00, 0.03),$$

we have

$$\sigma_{FT} = 2.192 > 0.808 = \sigma_{ST}.$$

However, for

$$(a_1, b_1) = (0.02, 0.02) \quad \text{and} \quad (a_2, b_2) = (0.00, 0.10),$$

we obtain

$$\sigma_{FT} = 0.400 < 2.600 = \sigma_{ST}.$$

□

Since the trimmed estimators $(\hat{\sigma}_T, \hat{\sigma}_T)$ in Eq. (29) are derived from Eq. (27), it is guaranteed in theory that one of the solutions for σ from the \pm branch must be positive. However, in finite samples, it is possible that $\hat{\sigma}_T < 0$, in which case the proposed trimmed L -moment estimation fails. Thus, to determine the appropriate sign of $\hat{\sigma}_T$ in Eq. (29), the following strategy is proposed. First, as established in Proposition 1, it holds theoretically that $T_2 - \eta_r T_1^2 \geq 0$. Therefore, assuming $(\hat{T}_2 - \eta_r \hat{T}_1^2)^{1/2} \geq 0$, we consider

$$\hat{\sigma}_{FT} = \frac{1}{\sqrt{\eta(a_1, \bar{b}_2)}} (\hat{T}_2 - \eta_r \hat{T}_1^2)^{1/2} \quad \text{and} \quad \hat{\sigma}_{ST} = \frac{\hat{T}_1 (c_1(a_1, \bar{b}_1) - c_1(a_2, \bar{b}_2))}{\eta(a_1, \bar{b}_2)}. \quad (34)$$

But for $a_1 \neq a_2$ or $b_1 \neq b_2$, it is possible to have $\hat{T}_2 - \eta_r \hat{T}_1^2 < 0$, i.e., $\hat{T}_2/\hat{T}_1^2 < \eta_r$, and in that case we consider

$$\hat{\sigma}_{FT} = \frac{1}{\sqrt{\eta(a_1, \bar{b}_2)}} (\left| \hat{T}_2 - \eta_r \hat{T}_1^2 \right|)^{1/2} \quad \text{and} \quad \hat{\sigma}_{ST} = \frac{\hat{T}_1 (c_1(a_1, \bar{b}_1) - c_1(a_2, \bar{b}_2))}{\eta(a_1, \bar{b}_2)}. \quad (35)$$

Thus, for location-scale models, it is guaranteed that $\hat{\sigma}_{FT} \geq 0$. However, $\hat{\sigma}_{ST} \in \mathbb{R}$.

If $\hat{\sigma}_{FT} < \hat{\sigma}_{ST}$, we define $\hat{\sigma}_- := -\hat{\sigma}_{FT} + \hat{\sigma}_{ST} > 0$. Similarly, if $\hat{\sigma}_{FT} > |\hat{\sigma}_{ST}|$, we define $\hat{\sigma}_+ := \hat{\sigma}_{FT} + \hat{\sigma}_{ST} > 0$. Finally, if $\hat{\sigma}_{FT} \leq |\hat{\sigma}_{ST}|$ and $\hat{\sigma}_{ST} \leq 0$, then the method fails to produce a nonnegative estimate of $\hat{\sigma}_T \geq 0$.

- If $a_1 = a_2 = a$ and $b_1 = b_2 = b$, then it follows that $\eta(a_1, \bar{b}_2) = \eta(a_2, \bar{b}_2)$, that is, $\eta_r = 1$. Also, $c_1(a_1, \bar{b}_1) - c_1(a_2, \bar{b}_2) = 0$. Thus,

$$\hat{\sigma}_T = \hat{\sigma}_+ = \left(\frac{\hat{T}_2 - \hat{T}_1^2}{c_2(a, \bar{b}) - c_1(a, \bar{b})^2} \right)^{1/2},$$

Algorithm 1: Trimmed Estimation of $(\hat{\theta}_T, \hat{\sigma}_T)$ in Location-Scale Models

Input: Sample data and trimming proportions $(a_1, b_1), (a_2, b_2)$ satisfying (25) or (31).

Output: Trimmed estimator vector $(\hat{\theta}_T, \hat{\sigma}_T)$.

```

1: Compute;
2:    $\hat{T}_1$  and  $\hat{T}_2$  from Eq. (26);
3:    $c_1(a_1, \bar{b}_1)$ ,  $c_1(a_2, \bar{b}_2)$ , and  $c_2(a_2, \bar{b}_2)$  from Eq. (28);
4:    $\eta(a_1, \bar{b}_2)$ ,  $\eta(a_2, \bar{b}_2)$ , and  $\eta_r$  from Eq. (30);
5:    $\hat{\sigma}_{FT}$  and  $\hat{\sigma}_{ST}$  from Eq. (34) or Eq. (35);
6:    $\hat{\sigma}_{MLE}$  from Eq. (36);
7: Set  $\hat{\sigma}_+ \leftarrow \hat{\sigma}_{FT} + \hat{\sigma}_{ST}$  and  $\hat{\sigma}_- \leftarrow -\hat{\sigma}_{FT} + \hat{\sigma}_{ST}$ ;
8: if  $a_1 = a_2$  and  $b_1 = b_2$  then
9:    $\hat{\sigma}_{ST} \leftarrow 0$ , resulting in  $\hat{\sigma}_T \leftarrow \hat{\sigma}_{FT}$ ;
10:  return  $\hat{\sigma}_T$ ;
11: end
12: else if  $(a_2 \leq a_1 \text{ and } b_1 \leq b_2)$  or  $(a_1 \leq a_2 \text{ and } b_2 \leq b_1)$  then
13:   if  $\max\{\hat{\sigma}_-, \hat{\sigma}_+\} \leq 0$  then
14:     /* Exit and update trimming proportions to ensure  $\hat{\sigma}_T > 0$ . */
15:     Ensure  $\max\{\hat{\sigma}_-, \hat{\sigma}_+\} > 0$ ;
16:   end
17:   else if  $\hat{\sigma}_- \leq 0$  and  $\hat{\sigma}_+ > 0$  then
18:      $\hat{\sigma}_T \leftarrow \hat{\sigma}_+$ ;
19:   end
20:   else if  $\hat{\sigma}_- > 0$  and  $\hat{\sigma}_+ \leq 0$  then
21:      $\hat{\sigma}_T \leftarrow \hat{\sigma}_-$ ;
22:   end
23:   else if  $\min\{\hat{\sigma}_-, \hat{\sigma}_+\} \geq 0$  then
24:     if  $|\hat{\sigma}_- - \hat{\sigma}_{MLE}| < |\hat{\sigma}_+ - \hat{\sigma}_{MLE}|$  then
25:        $\hat{\sigma}_T \leftarrow \hat{\sigma}_-$ 
26:     end
27:     else
28:        $\hat{\sigma}_T \leftarrow \hat{\sigma}_+$ ;
29:     end
30:   end
31:   return  $\hat{\sigma}_T$ ;
32:    $\hat{\theta}_T \leftarrow \hat{T}_1 - c_1(a_1, \bar{b}_1) \hat{\sigma}_T$ ;
33: return  $(\hat{\theta}_T, \hat{\sigma}_T)$ ;

```

and this result coincides exactly with the solution presented in Eq. (2.7) of [Brazauskas *et al.* \(2009\)](#), as expected.

- If $a_1 \neq a_2$ or $b_1 \neq b_2$, selecting the appropriate sign in Eq. (29) becomes nontrivial. For either trimming inequality (25) or (31), we begin by computing the standard deviation of the full

sample X_1, X_2, \dots, X_n as

$$\hat{\sigma}_{\text{MLE}} = \sqrt{\frac{1}{n} \sum_{i=1}^n (X_i - \bar{X})^2}. \quad (36)$$

If $\max\{\hat{\sigma}_-, \hat{\sigma}_+\} \leq 0$, then there is no positive solution for the scale parameter σ . Otherwise, if $\hat{\sigma}_- \leq 0$ and $\hat{\sigma}_+ > 0$, then we simply assign $\hat{\sigma}_{\text{T}} = \hat{\sigma}_+$. Similarly, if $\hat{\sigma}_- > 0$ and $\hat{\sigma}_+ \leq 0$, then $\hat{\sigma}_{\text{T}} = \hat{\sigma}_-$. Finally, assuming $\min\{\hat{\sigma}_-, \hat{\sigma}_+\} \geq 0$, and following a rationale similar to that used in selecting a decision threshold in logistic classification, we choose between $\hat{\sigma}_-$ and $\hat{\sigma}_+$ based on their proximity to the maximum likelihood estimate. That is,

$$\hat{\sigma}_{\text{T}} = \begin{cases} \hat{\sigma}_-, & \text{if } |\hat{\sigma}_- - \hat{\sigma}_{\text{MLE}}| < |\hat{\sigma}_+ - \hat{\sigma}_{\text{MLE}}|, \\ \hat{\sigma}_+, & \text{if } |\hat{\sigma}_+ - \hat{\sigma}_{\text{MLE}}| \leq |\hat{\sigma}_- - \hat{\sigma}_{\text{MLE}}|. \end{cases} \quad (37)$$

A formal procedure for estimating the parameter vector $(\hat{\theta}_{\text{T}}, \hat{\sigma}_{\text{T}})$ is summarized in Algorithm 1.

Note 6. For $(a_1, b_1) = (a_2, b_2) = (a, b)$, it follows that $\eta(a_1, \bar{b}_2) = \eta(a_2, \bar{b}_2)$, that is, $\eta_r = 1$, and the result given by Eq. (29) coincides exactly with the solution presented in Eq. (2.7) of [Brazauskas et al. \(2009\)](#), as expected. \square

From Theorem 1 along with Eqs. (22) and (24), we calculate the entries of the covariance matrix $\Sigma_{\text{T}} = [\sigma_{ij}^2]_{i,j=1}^2$ as below:

$$\begin{aligned} \sigma_{11}^2 &= \Gamma(1, 1)V(1, 1) \\ &= \Gamma(1, 1) \int_{a_1}^{\bar{b}_1} \int_{a_1}^{\bar{b}_1} K(w, v) H'_1(w) H'_1(v) dv dw \\ &= \sigma^2 \Gamma(1, 1) \int_{a_1}^{\bar{b}_1} \int_{a_1}^{\bar{b}_1} K(w, v) dF_0^{-1}(v) dF_0^{-1}(w) dv dw \\ &= \sigma^2 \Lambda_{111}, \end{aligned} \quad (38)$$

$$\begin{aligned} \sigma_{12}^2 &= \Gamma(1, 2)V(1, 2) \\ &= \Gamma(1, 2) \int_{a_1}^{\bar{b}_1} \int_{a_2}^{\bar{b}_2} K(w, v) H'_1(w) H'_2(v) dv dw \\ &= \Gamma(1, 2) \left\{ 2\theta\sigma^2 \int_{a_1}^{\bar{b}_1} \int_{a_2}^{\bar{b}_2} K(w, v) dF_0^{-1}(v) dF_0^{-1}(w) dv dw \right. \\ &\quad \left. + 2\sigma^3 \int_{a_1}^{\bar{b}_1} \int_{a_2}^{\bar{b}_2} K(w, v) F_0^{-1}(v) dF_0^{-1}(v) dF_0^{-1}(w) dv dw \right\} \\ &= 2\theta\sigma^2 \Lambda_{121} + 2\sigma^3 \Lambda_{122}, \end{aligned} \quad (39)$$

$$\sigma_{22}^2 = \Gamma(2, 2)V(2, 2)$$

$$\begin{aligned}
&= \Gamma(2, 2) \int_{a_2}^{\bar{b}_2} \int_{a_2}^{\bar{b}_2} K(w, v) H'_2(w) H'_2(v) dv dw \\
&= \Gamma(2, 2) \left\{ 4\theta^2 \sigma^2 \int_{a_2}^{\bar{b}_2} \int_{a_2}^{\bar{b}_2} K(w, v) dF_0^{-1}(v) dF_0^{-1}(w) dv dw \right. \\
&\quad + 8\theta \sigma^3 \int_{a_2}^{\bar{b}_2} \int_{a_2}^{\bar{b}_2} K(w, v) F_0^{-1}(w) dF_0^{-1}(v) dF_0^{-1}(w) dv dw \\
&\quad \left. + 4\sigma^4 \int_{a_2}^{\bar{b}_2} \int_{a_2}^{\bar{b}_2} K(w, v) F_0^{-1}(w) F_0^{-1}(v) dF_0^{-1}(v) dF_0^{-1}(w) dv dw \right\} \\
&= 4\theta^2 \sigma^2 \Lambda_{221} + 8\theta \sigma^3 \Lambda_{222} + 4\sigma^4 \Lambda_{223}, \tag{40}
\end{aligned}$$

where the notations Λ_{ijk} , for $1 \leq i, j \leq 2$ and $1 \leq k \leq 3$ do not depend on the parameters to be estimated and are listed in Appendix B.

Note 7. For the equal trimming proportions $(a_1, b_1) = (a_2, b_2) = (a, b)$, we have

$$\Lambda_{111} = \Lambda_{121} = \Lambda_{221} = c_1^*, \quad \Lambda_{122} = \Lambda_{222} = c_2^*, \quad \text{and} \quad \Lambda_{223} = c_3^*,$$

where the notations c_i^* , $i = 1, 2, 3$ can be found in Brazauskas et al. (2009). \square

As defined in Corollary 2, the entries of the matrix $\mathbf{D}_T = [d_{ij}]_{i,j=1}^2$, are obtained by differentiating the functions g_i from Eqs. (29):

$$d_{11} = 1 - c_1(a_1, \bar{b}_1) \frac{\partial g_2}{\partial \hat{T}_1}, \quad d_{12} = -c_1(a_1, \bar{b}_1) \frac{\partial g_2}{\partial \hat{T}_2}.$$

The two entries d_{21} and d_{22} depend on the sign of the $\hat{\sigma}_T$ as seen in Eq. (37). That is, if $\hat{\sigma}_T = \hat{\sigma}_-$, then

$$d_{21}^- = \frac{\partial g_2}{\partial \hat{T}_1} = \frac{\eta_r \hat{T}_1}{\sqrt{\eta(a_1, \bar{b}_2)}} \left(\hat{T}_2 - \eta_r \hat{T}_1^2 \right)^{-\frac{1}{2}} + \frac{c_1(a_1, \bar{b}_1) - c_1(a_2, \bar{b}_2)}{\eta(a_1, \bar{b}_2)}, \tag{41}$$

$$d_{22}^- = \frac{\partial g_2}{\partial \hat{T}_2} = \frac{-1}{2 \sqrt{\eta(a_1, \bar{b}_2)}} \left(\hat{T}_2 - \eta_r \hat{T}_1^2 \right)^{-\frac{1}{2}}. \tag{42}$$

And, if $\hat{\sigma}_T = \hat{\sigma}_+$, then

$$d_{21}^+ = \frac{\partial g_2}{\partial \hat{T}_1} = \frac{-\eta_r \hat{T}_1}{\sqrt{\eta(a_1, \bar{b}_2)}} \left(\hat{T}_2 - \eta_r \hat{T}_1^2 \right)^{-\frac{1}{2}} + \frac{c_1(a_1, \bar{b}_1) - c_1(a_2, \bar{b}_2)}{\eta(a_1, \bar{b}_2)}, \tag{43}$$

$$d_{22}^+ = \frac{\partial g_2}{\partial \hat{T}_2} = \frac{1}{2 \sqrt{\eta(a_1, \bar{b}_2)}} \left(\hat{T}_2 - \eta_r \hat{T}_1^2 \right)^{-\frac{1}{2}}. \tag{44}$$

Lemma 1. Define

$$\mathbf{D}_T^- = \begin{bmatrix} d_{11} & d_{12} \\ d_{21}^- & d_{22}^- \end{bmatrix} \quad \text{and} \quad \mathbf{D}_T^+ = \begin{bmatrix} d_{11} & d_{12} \\ d_{21}^+ & d_{22}^+ \end{bmatrix},$$

then it follows that $\det(\mathbf{D}_T^-) + \det(\mathbf{D}_T^+) = 0$.

We will be using the Jacobian matrix \mathbf{D}_T to compute the ARE as presented in Eq. (17), where $\Sigma_c = \mathbf{D}_T \Sigma_T \mathbf{D}_T'$. Since both matrices \mathbf{D}_T and Σ_T are 2×2 square matrices, it follows from Schott (2017, Theorem 1.7) that $\det(\mathbf{D}_T \Sigma_T \mathbf{D}_T') = (\det(\mathbf{D}_T))^2 \det(\Sigma_T)$. Therefore, by the property established in Lemma 1, choosing either \mathbf{D}_T^- or \mathbf{D}_T^+ for the Jacobian matrix \mathbf{D}_T does not affect the final ARE calculation. Thus, without loss of generality, we proceed with $\mathbf{D}_T = \mathbf{D}_T^+$.

Further, define

$$\Omega := |\sigma(c_2(a_2, \bar{b}_2) - c_1(a_1, \bar{b}_1)c_1(a_2, \bar{b}_2)) + \theta(c_1(a_2, \bar{b}_2) - c_1(a_1, \bar{b}_1))|,$$

then it follows that

$$\begin{aligned} d_{11} &= \frac{\partial g_1}{\partial \widehat{T}_1} \Big|_{(T_1, T_2)} = \frac{\eta_r}{\Omega} [\sigma c_1^2(a_1, \bar{b}_1) + \theta c_1(a_1, \bar{b}_1)] + \frac{c_2(a_2, \bar{b}_2) - c_1(a_1, \bar{b}_1)c_1(a_2, \bar{b}_2)}{\eta(a_1, \bar{b}_2)}, \\ d_{12} &= \frac{\partial g_1}{\partial \widehat{T}_2} \Big|_{(T_1, T_2)} = -\frac{c_1(a_1, \bar{b}_1)}{2\Omega}, \\ d_{21} &= \frac{\partial g_2}{\partial \widehat{T}_1} \Big|_{(T_1, T_2)} = -\frac{1}{\Omega \eta(a_1, \bar{b}_2)} [\Omega(c_1(a_2, \bar{b}_2) - c_1(a_1, \bar{b}_1)) + (\theta + \sigma c_1(a_1, \bar{b}_1)) \eta(a_2, \bar{b}_2)], \\ d_{22} &= \frac{\partial g_2}{\partial \widehat{T}_2} \Big|_{(T_1, T_2)} = \frac{1}{2\Omega}. \end{aligned}$$

Therefore, we get

$$(\widehat{\theta}_T, \widehat{\sigma}_T) \sim \mathcal{AN}\left((\theta, \sigma), \frac{1}{n} \mathbf{S}_T\right), \quad \text{where} \quad \mathbf{S}_T = \mathbf{D}_T \Sigma_T \mathbf{D}_T'. \quad (45)$$

Thus, from Eq. (17) and Eq. (45), we have

$$\text{ARE}\left(\left(\widehat{\theta}_T, \widehat{\sigma}_T\right), \left(\widehat{\theta}_{\text{MLE}}, \widehat{\sigma}_{\text{MLE}}\right)\right) = (\det(\mathbf{S}_{\text{MLE}}) / \det(\mathbf{S}_T))^{0.5}. \quad (46)$$

Numerical values of the AREs, computed using Eq. (46), are reported in Table 1 for various trimming proportions satisfying inequality (25), under a normal distribution with fixed $\sigma = 3$ and varying location parameter θ . The corresponding ARE curve is shown in the top panel of Figure 1 (solid black line) for trimming proportions $(a_1, b_1) = (0.05, 0.05)$ and $(a_2, b_2) = (0.00, 0.10)$.

Table 1: From $N(\theta, \sigma^2 = 3^2)$, and we vary the location parameter θ . Inequality used (25).

Proportions		θ									
(a_1, b_1)	(a_2, b_2)	-25	-15	-10	-5	0	5	10	15	25	
(0.02, 0.02)	(0.02, 0.02)	0.943	0.943	0.943	0.943	0.943	0.943	0.943	0.943	0.943	
(0.02, 0.02)	(0.00, 0.04)	0.903	0.931	0.944	0.952	0.946	0.903	0.794	0.599	0.121	
(0.05, 0.05)	(0.05, 0.05)	0.872	0.872	0.872	0.872	0.872	0.872	0.872	0.872	0.872	
(0.05, 0.05)	(0.00, 0.10)	0.878	0.890	0.897	0.901	0.883	0.746	0.206	0.334	0.650	
(0.10, 0.10)	(0.10, 0.10)	0.769	0.769	0.769	0.769	0.769	0.769	0.769	0.769	0.769	
(0.10, 0.10)	(0.00, 0.20)	0.851	0.850	0.849	0.842	0.805	0.330	0.684	0.797	0.831	
(0.15, 0.15)	(0.15, 0.15)	0.676	0.676	0.676	0.676	0.676	0.676	0.676	0.676	0.676	
(0.15, 0.15)	(0.00, 0.30)	0.812	0.809	0.806	0.797	0.753	0.249	0.788	0.810	0.815	

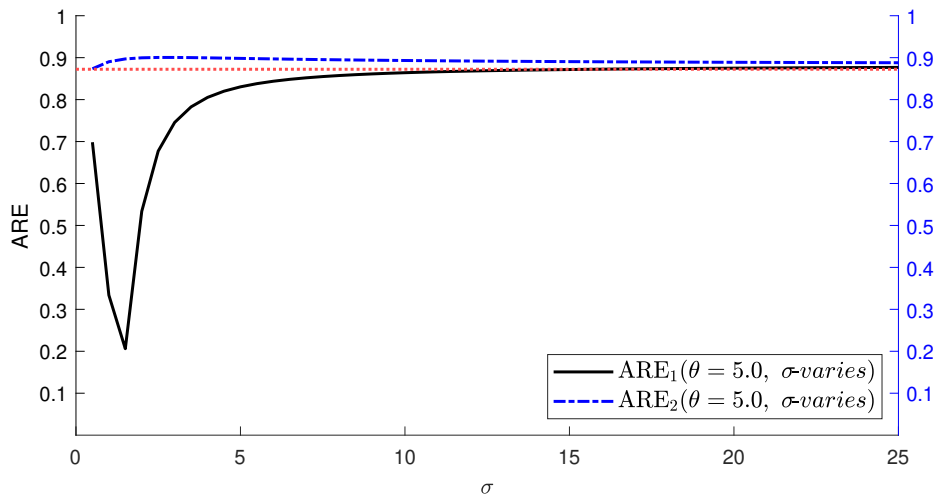
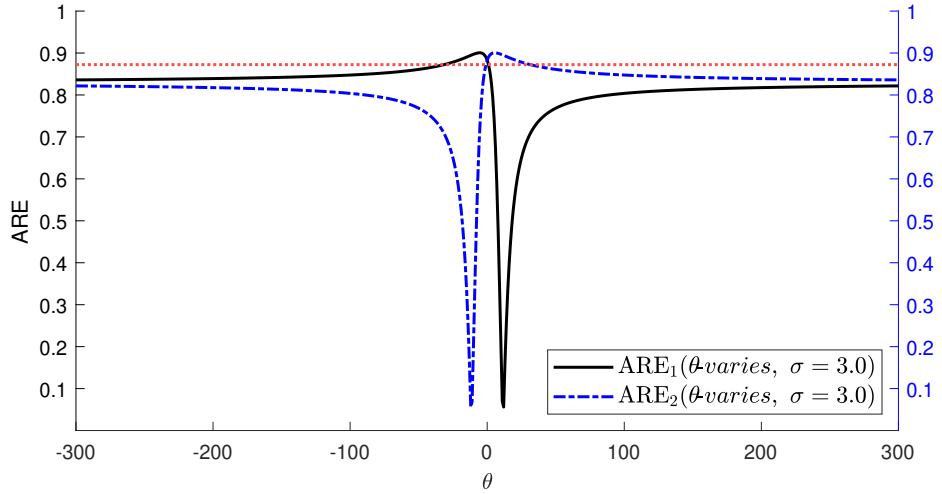
Due to space constraints, we omit the ARE table for the reverse setting where $\theta = 5$ is fixed and σ varies, but the associated curve is displayed in the bottom panel of Figure 31 (solid black line), using the same trimming configuration.

Although similar tables can be generated for other trimming proportions under inequality (31), we include only the corresponding ARE curves. For the case with $\sigma = 3$ fixed and varying θ , the top panel of Figure 31 shows the result as a dash-dot blue curve. Likewise, when $\theta = 5$ is fixed and σ varies, the bottom panel presents the corresponding ARE curve using the same line style.

Several key findings emerge from Table 1 and Figure 1. In Figure 1, the horizontal red dotted line represents the ARE value obtained from a normal distribution using identical trimming proportions for both moments, i.e., $(a_1, b_1) = (a_2, b_2) = (0.05, 0.05)$. When the location parameter θ is close to zero, the AREs corresponding to trimming inequalities (25) or (31) exceed those obtained under equal trimming for both moments. This observation supports the primary motivation of this study: when the data and underlying model are approximately symmetric about the origin, applying the same trimming to both moments can unintentionally exclude different sets of observations, thereby reducing efficiency (see Note 3). In contrast, under inequalities (25) or (31), asymmetric trimming may preserve informative observations for specific moments, leading to higher efficiency.

However, when $|\theta|$ becomes large, trimming inequalities (25) and (31) do not trim the same data points across moments, unlike equal trimming, which can lead to reduced efficiency and lower AREs.

Table 1 also illustrates that the ARE generally decreases with increasing trimming proportions. Nonetheless, the decline in ARE is slower under asymmetric trimming (inequalities (25) and (31)) compared to equal trimming. In other words, the ARE curves in Figure 1 exhibit similar shapes



$$\begin{aligned}
ARE_1(\theta\text{-varies}, \sigma = 3) &= ARE(\theta\text{-varies}, \sigma = 3, (a_1, b_1) = (0.05, 0.05), (a_2, b_2) = (0.00, 0.10)) \\
ARE_2(\theta\text{-varies}, \sigma = 3) &= ARE(\theta\text{-varies}, \sigma = 3, (a_1, b_1) = (0.05, 0.05), (a_2, b_2) = (0.10, 0.00)) \\
ARE_1(\theta = 5, \sigma\text{-varies}) &= ARE(\theta = 5, \sigma\text{-varies}, (a_1, b_1) = (0.05, 0.05), (a_2, b_2) = (0.00, 0.10)) \\
ARE_2(\theta = 5, \sigma\text{-varies}) &= ARE(\theta = 5, \sigma\text{-varies}, (a_1, b_1) = (0.05, 0.05), (a_2, b_2) = (0.10, 0.00))
\end{aligned}$$

Figure 1: Normal ARE curves under trimming inequalities (25) or (31).

across trimming levels, but their height decreases more gradually under asymmetric configurations, suggesting a more stable robustness-efficiency trade-off.

Importantly, the lowest ARE values occur when $T_2 - \eta_r T_1^2 \rightarrow 0^+$, indicating near-singularity in the scale estimation formula. If the true values of θ and σ result in $T_2 - \eta_r T_1^2 \rightarrow 0^+$, this may lead to $\widehat{T}_2 - \eta_r \widehat{T}_1^2 < 0$, or equivalently, $\widehat{T}_2/\widehat{T}_1^2 < \eta_r$, making the estimation unstable. For instance, with fixed $\theta = 5$ and varying σ (Figure 1, bottom panel), the ARE drops sharply as $T_2 - \eta_r T_1^2 \rightarrow 0^+$,

with the trimming inequality (25). Otherwise, for both trimming inequalities, the ARE stabilizes as σ increases, showing that the MTM method performs reliably even with widely dispersed or contaminated data.

For a fixed negative value, such as $\theta = -5$, the ARE curves in Figure 1 (bottom panel) retain their shape, but the roles of the black and blue curves are reversed.

3.2 Fréchet Model

As a member of the location-scale family of distributions, the pdf and cdf are, respectively, given by

$$\begin{aligned} f(x) &= \frac{\alpha}{\sigma} \left(\frac{x-\theta}{\sigma} \right)^{-(\alpha+1)} \exp \left[- \left(\frac{\sigma}{x-\theta} \right)^\alpha \right]; \quad x > \theta, \\ F(x) &= \exp \left[- \left(\frac{\sigma}{x-\theta} \right)^\alpha \right], \end{aligned}$$

where $-\infty < \theta < \infty$, $\sigma > 0$, and $\alpha > 0$ are, respectively, the location, scale, and shape parameters. But to investigate the performance of general MTM for strictly positive distribution, we set the location parameter $\theta = 0$. Thus, we are left to estimate the scale parameter, σ , and the shape parameter, α , of the distribution. Furthermore, for ease of estimation, instead of directly estimating the shape parameter α , we estimate the *tail index*, defined as its reciprocal, $\beta := 1/\alpha$. The moments and quantile functions are given by

$$\mathbb{E} [X^k] = \sigma^k \Gamma(1 - k\beta); \quad k\beta < 1, \quad \text{and} \quad F^{-1}(u) = \sigma (-\log(u))^{-\beta}.$$

Unlike for location-scale member, we take the two functions

$$h_1(x) = \log(x) \quad \text{and} \quad h_2(x) = (\log(x))^2. \quad (47)$$

Thus, with $H_j := h_j \circ F^{-1}$, it follows that

$$H_1(u) = h_1(F^{-1}(u)) = \log(\sigma) - \beta \log(-\log(u)), \quad (48)$$

$$\implies H'_1(u) = -\frac{\beta}{u \log(u)}, \quad (49)$$

$$H_2(u) = h_2(F^{-1}(u)) = (\log(\sigma))^2 - 2\beta \log(\sigma) \log(-\log(u)) + \beta^2 (\log(-\log(u)))^2 \quad (50)$$

$$\implies H'_2(u) = \frac{2\beta^2 \log(-\log(u))}{u \log(u)} - \frac{2\beta \log(\sigma)}{u \log(u)} = \frac{2\beta}{u \log(u)} (\beta \log(-\log(u)) - \log(\sigma)). \quad (51)$$

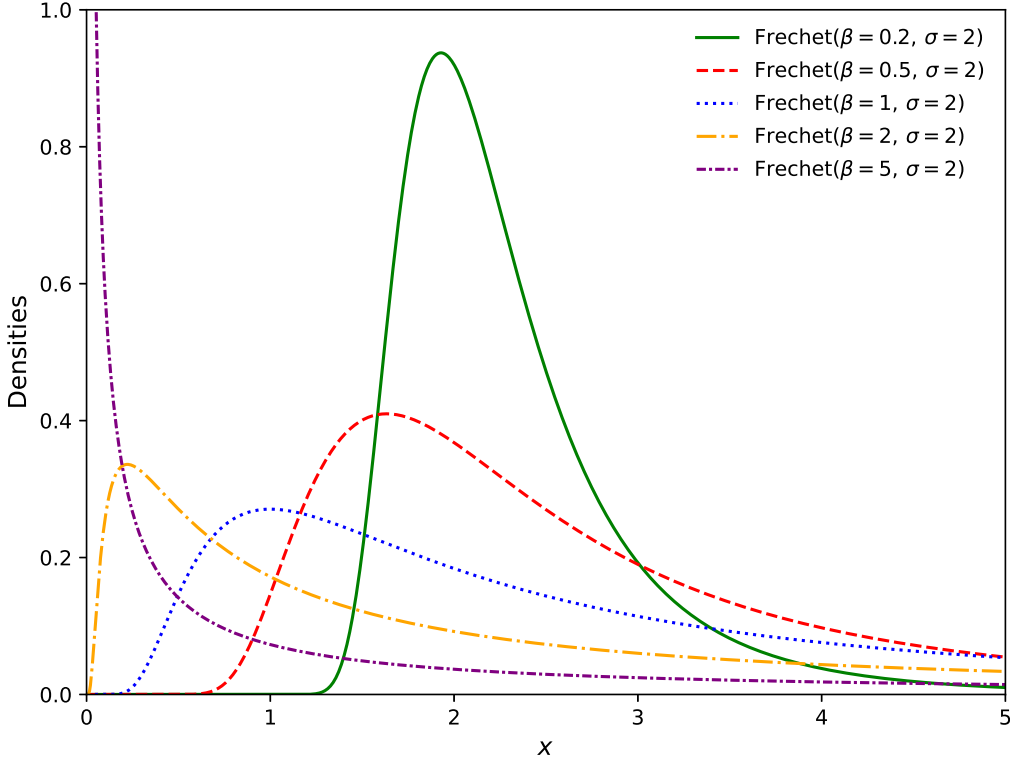


Figure 2: Frechet Densities. A larger β (i.e., a smaller shape parameter α) implies a heavier tail. This is because $S(x; \sigma, \beta_1) \leq S(x; \sigma, \beta_2)$ for all $x \geq 0$ and $\beta_1 \leq \beta_2$, where S denotes the survival function.

With the trimming proportions (a_1, b_1) and (a_2, b_2) as given in (25), then from Eq. (1), the first two sample trimmed-moments are given by:

$$\begin{cases} \hat{T}_1 = \frac{1}{n - \lfloor na_1 \rfloor - \lfloor nb_1 \rfloor} \sum_{i=\lfloor na_1 \rfloor + 1}^{n - \lfloor nb_1 \rfloor} h_1(X_{i:n}) = \frac{1}{n - \lfloor na_1 \rfloor - \lfloor nb_1 \rfloor} \sum_{i=\lfloor na_1 \rfloor + 1}^{n - \lfloor nb_1 \rfloor} \log(X_{i:n}), \\ \hat{T}_2 = \frac{1}{n - \lfloor na_2 \rfloor - \lfloor nb_2 \rfloor} \sum_{i=\lfloor na_2 \rfloor + 1}^{n - \lfloor nb_2 \rfloor} h_2(X_{i:n}) = \frac{1}{n - \lfloor na_2 \rfloor - \lfloor nb_2 \rfloor} \sum_{i=\lfloor na_2 \rfloor + 1}^{n - \lfloor nb_2 \rfloor} (\log(X_{i:n}))^2. \end{cases} \quad (52)$$

The corresponding first two population trimmed-moments using Eq. (2) takes the form:

$$\begin{cases} T_1 = \frac{1}{1 - a_1 - b_1} \int_{a_1}^{\bar{b}_1} H_1(u) du = \log(\sigma) - \beta \kappa_1(a_1, \bar{b}_1), \\ T_2 = \frac{1}{1 - a_2 - b_2} \int_{a_2}^{\bar{b}_2} H_2(u) du = (\log(\sigma))^2 - 2\beta \log(\sigma) \kappa_1(a_2, \bar{b}_2) + \beta^2 \kappa_2(a_2, \bar{b}_2), \end{cases} \quad (53)$$

where

$$\kappa_k(a, b) := \frac{1}{b - a} \int_a^b [\Delta(u)]^k du, \quad \Delta(u) := \log(-\log(u)), \quad k \geq 1, \quad (54)$$

do not depend on the parameters β and σ to be estimated.

Setting $(T_1, T_2) = (\widehat{T}_1, \widehat{T}_2)$ from Eqs. (52) and (53), and solving for β and σ , we get the explicit trimmed L -estimators as

$$\begin{cases} \widehat{\beta}_T = \frac{\pm 1}{\sqrt{\zeta(a_1, \bar{b}_2)}} (\widehat{T}_2 - \zeta_r \widehat{T}_1^2)^{1/2} + \frac{\widehat{T}_1 (\kappa_1(a_2, \bar{b}_2) - \kappa_1(a_1, \bar{b}_1))}{\zeta(a_1, \bar{b}_2)} =: g_1(\widehat{T}_1, \widehat{T}_2), \\ \widehat{\sigma}_T = \exp \left\{ \widehat{T}_1 + \widehat{\beta}_T \kappa_1(a_1, \bar{b}_1) \right\} =: g_2(\widehat{T}_1, \widehat{T}_2), \end{cases} \quad (55)$$

where, as in Eq. (30), and for $1 \leq i, j \leq 2$, we define

$$\zeta(a_i, \bar{b}_j) := \kappa_1^2(a_i, \bar{b}_i) - 2\kappa_1(a_i, \bar{b}_i)\kappa_1(a_j, \bar{b}_j) + \kappa_2(a_j, \bar{b}_j), \quad 1 \leq i, j \leq 2, \quad \zeta_r := \frac{\zeta(a_j, \bar{b}_j)}{\zeta(a_i, \bar{b}_j)}. \quad (56)$$

We now summarize some results, similar to those in Proposition 1, in Corollary 2.

Corollary 2. *With the trimming proportions (a_i, b_i) and (a_j, b_j) satisfying the inequality (8), it follows that*

$$(i) \quad \zeta(a_i, \bar{b}_j) = \kappa_1^2(a_i, \bar{b}_i) - 2\kappa_1(a_i, \bar{b}_i)\kappa_1(a_j, \bar{b}_j) + \kappa_2(a_j, \bar{b}_j) > 0.$$

$$(ii) \quad \kappa_k(a_i, \bar{b}_i) \leq \kappa_k(a_j, \bar{b}_j), \text{ for any odd positive integer } k.$$

$$(iii) \quad 0 < \zeta_r = \frac{\zeta(a_j, \bar{b}_j)}{\zeta(a_i, \bar{b}_j)} \leq 1.$$

$$(iv) \quad \kappa_2(a_j, \bar{b}_j) \geq \zeta_r \kappa_1^2(a_i, \bar{b}_i).$$

$$(v) \quad T_2 - \zeta_r T_1^2 \geq 0.$$

Proof. See Appendix A. □

Similar to Corollary 1, we have the following result.

Corollary 3. *Under the trimming inequality (15), that is, (31) for Fréchet model, all results of Corollary 2 remain valid except for Part (ii), which instead takes the form $\kappa_k(a_i, \bar{b}_i) \geq \kappa_k(a_j, \bar{b}_j)$, for any odd positive integer k .*

Note 8. Define

$$\beta_{FT} = \frac{1}{\sqrt{\zeta(a_1, \bar{b}_2)}} (T_2 - \zeta_r T_1^2)^{1/2} \quad \text{and} \quad \beta_{ST} = \frac{T_1 (\kappa_1(a_2, \bar{b}_2) - \kappa_1(a_1, \bar{b}_1))}{\zeta(a_1, \bar{b}_2)}. \quad (57)$$

Similarly as mentioned in Note 5, under the trimming inequality (25), a consistent directional relationship between β_{FT} and β_{ST} is not guaranteed.

For illustration, consider $X \sim \text{Fr\'echet}(\beta = 2, \sigma = 3)$. Then, for

$$(a_1, b_1) = (0.02, 0.02) \quad \text{and} \quad (a_2, b_2) = (0.00, 0.03),$$

we have

$$\beta_{FT} = 1.860 > 0.139 = \beta_{ST}.$$

However, for

$$(a_1, b_1) = (0.02, 0.02) \quad \text{and} \quad (a_2, b_2) = (0.00, 0.20),$$

we obtain

$$\beta_{FT} = 0.738 < 1.262 = \beta_{ST}.$$

□

As in Section 3.1, the trimmed estimators $(\hat{\beta}_T, \hat{\sigma}_T)$ in Eq. (55) are derived from Eq. (53), ensuring that one of the solutions from the \pm branch for β is theoretically positive. However, for finite samples, it is possible that $\hat{\beta}_T < 0$, in which case the proposed trimmed L -moment estimation is invalid. To determine the correct sign of $\hat{\beta}_T$, in Eq. (55), we adopt the following strategy. As established in Corollary 2, it holds that $T_2 - \zeta_r T_1^2 \geq 0$. Therefore, assuming $(\hat{T}_2 - \eta_r \hat{T}_1^2)^{1/2} \geq 0$, we consider

$$\hat{\beta}_{FT} = \frac{1}{\sqrt{\zeta(a_1, \bar{b}_2)}} (\hat{T}_2 - \zeta_r \hat{T}_1^2)^{1/2} \quad \text{and} \quad \hat{\beta}_{ST} = \frac{\hat{T}_1 (\kappa_1(a_2, \bar{b}_2) - \kappa_1(a_1, \bar{b}_1))}{\zeta(a_1, \bar{b}_2)}. \quad (58)$$

But for $a_1 \neq a_2$ or $b_1 \neq b_2$, it is possible to have $\hat{T}_2 - \zeta_r \hat{T}_1^2 < 0$, i.e., $\hat{T}_2/\hat{T}_1^2 < \zeta_r$, and in that case we consider

$$\hat{\beta}_{FT} = \frac{\pm 1}{\sqrt{\zeta(a_1, \bar{b}_2)}} (\left| \hat{T}_2 - \zeta_r \hat{T}_1^2 \right|)^{1/2} \quad \text{and} \quad \hat{\beta}_{ST} = \frac{\hat{T}_1 (\kappa_1(a_2, \bar{b}_{21}) - \kappa_1(a_1, \bar{b}_1))}{\zeta(a_1, \bar{b}_2)}. \quad (59)$$

Therefore, for Fr\'echet models, we have $\hat{\beta}_{FT} \geq 0$, by construction. In contrast, $\hat{\beta}_{ST}$ may take any real value, i.e., $\hat{\beta}_{ST} \in \mathbb{R}$.

If $\hat{\beta}_{FT} < \hat{\beta}_{ST}$, we define $\hat{\beta}_- := -\hat{\beta}_{FT} + \hat{\beta}_{ST} > 0$. Similarly, if $\hat{\beta}_{FT} > |\hat{\beta}_{ST}|$, we define $\hat{\beta}_+ := \hat{\beta}_{FT} + \hat{\beta}_{ST} > 0$. Finally, if $\hat{\beta}_{FT} \leq |\hat{\beta}_{ST}|$ and $\hat{\beta}_{ST} \leq 0$, then the method fails to yield a nonnegative estimate of $\hat{\beta}_T \geq 0$.

Algorithm 2: Trimmed Estimation of $(\hat{\beta}_T, \hat{\sigma}_T)$ in Fréchet Model

Input: Sample data and trimming proportions $(a_1, b_1), (a_2, b_2)$ satisfying (25) or (31).

Output: Trimmed estimator vector $(\hat{\beta}_T, \hat{\sigma}_T)$.

```

1: Compute;
2:    $\hat{T}_1$  and  $\hat{T}_2$  from Eq. (52);
3:    $\kappa_1(a_1, \bar{b}_1)$ ,  $\kappa_1(a_2, \bar{b}_2)$ , and  $\kappa_2(a_2, \bar{b}_2)$  from Eq. (54);
4:    $\zeta(a_1, \bar{b}_2)$ ,  $\zeta(a_2, \bar{b}_2)$ , and  $\zeta_r$  from Eq. (56);
5:    $\hat{\beta}_{FT}$  and  $\hat{\beta}_{ST}$  from Eq. (58) or Eq. (59);
6:    $\hat{\beta}_{MLE}$  from Eq. (60);
7: Set  $\hat{\beta}_+ \leftarrow \hat{\beta}_{FT} + \hat{\beta}_{ST}$  and  $\hat{\beta}_- \leftarrow -\hat{\beta}_{FT} + \hat{\beta}_{ST}$ ;
8: if  $a_1 = a_2$  and  $b_1 = b_2$  then
9:    $\hat{\beta}_{ST} \leftarrow 0$ , resulting in  $\hat{\beta}_T \leftarrow \hat{\beta}_{FT}$ ;
10:  return  $\hat{\beta}_T$ ;
11: end
12: else if  $(a_2 \leq a_1 \text{ and } b_1 \leq b_2)$  or  $(a_1 \leq a_2 \text{ and } b_2 \leq b_1)$  then
13:   if  $\max\{\hat{\beta}_-, \hat{\beta}_+\} \leq 0$  then
14:     /* Exit and update trimming proportions to ensure  $\hat{\beta}_T > 0$ . */
15:     Ensure  $\max\{\hat{\beta}_-, \hat{\beta}_+\} > 0$ ;
16:   end
17:   else if  $\hat{\beta}_- \leq 0$  and  $\hat{\beta}_+ > 0$  then
18:      $\hat{\beta}_T \leftarrow \hat{\beta}_+$ ;
19:   end
20:   else if  $\hat{\beta}_- > 0$  and  $\hat{\beta}_+ \leq 0$  then
21:      $\hat{\beta}_T \leftarrow \hat{\beta}_-$ ;
22:   end
23:   else if  $\min\{\hat{\beta}_-, \hat{\beta}_+\} \geq 0$  then
24:     if  $|\hat{\beta}_- - \hat{\beta}_{MLE}| < |\hat{\beta}_+ - \hat{\beta}_{MLE}|$  then
25:        $\hat{\beta}_T \leftarrow \hat{\beta}_-$ 
26:     end
27:     else
28:        $\hat{\beta}_T \leftarrow \hat{\beta}_+$ ;
29:     end
30:   end
31:   return  $\hat{\beta}_T$ ;
32:    $\hat{\sigma}_T \leftarrow \exp\{\hat{T}_1 + \hat{\beta}_T \kappa_1(a_1, \bar{b}_1)\}$ ;
33: return  $(\hat{\beta}_T, \hat{\sigma}_T)$ ;

```

- If $a_1 = a_2 = a$ and $b_1 = b_2 = b$, then it follows that $\zeta(a_1, \bar{b}_2) = \eta(a_2, \bar{b}_2)$, that is, $\zeta_r = 1$. Also,

$\kappa_1(a_1, \bar{b}_1) - \kappa_1(a_2, \bar{b}_2) = 0$. Thus,

$$\hat{\beta}_T = \hat{\beta}_+ = \left(\frac{\hat{T}_2 - \hat{T}_1^2}{\kappa_2(a, \bar{b}) - \kappa_1(a, \bar{b})^2} \right)^{1/2}.$$

- If $a_1 \neq a_2$ or $b_1 \neq b_2$, selecting the appropriate sign in Eq. (55) becomes nontrivial. To proceed, and following Nawa and Nadarajah (2025, Eq. (6)), the L -moment estimate of β is given by

$$\hat{\beta}_{LM} = \frac{\log(2) + \log(\sum_{i=1}^n (i-1)X_{i:n}) - \log(n(n-1)\bar{X})}{\log(2)},$$

but this closed-form expression is valid only if $\beta < 1$. Thus, instead of relying on this restricted formula, we treat β as a tunable parameter and estimate it using the method of maximum likelihood. Following Bücher and Segers (2018), $\hat{\beta}_{MLE}$ is the unique root of the strictly increasing function

$$\xi(\beta) = \beta + \sum_{i=1}^n x_i^{-1/\beta} \log(x_i) \left(\sum_{i=1}^n x_i^{-1/\beta} \right)^{-1} - n^{-1} \sum_{i=1}^n \log(x_i), \quad \text{i.e.,} \quad \xi(\hat{\beta}_{MLE}) = 0. \quad (60)$$

The maximum likelihood estimator of σ is given by

$$\hat{\sigma}_{MLE} = \left(\frac{1}{n} \sum_{i=1}^n x_i^{-1/\hat{\beta}_{MLE}} \right)^{-\hat{\beta}_{MLE}}. \quad (61)$$

If $\max\{\hat{\beta}_-, \hat{\beta}_+\} \leq 0$, there is no valid positive solution for the tail index parameter β . Otherwise, if $\hat{\beta}_- \leq 0$ and $\hat{\beta}_+ > 0$, we set $\hat{\beta}_T = \hat{\beta}_+$. Similarly, if $\hat{\beta}_- > 0$ and $\hat{\beta}_+ \leq 0$, we set $\hat{\beta}_T = \hat{\beta}_-$. Finally, if $\min\{\hat{\beta}_-, \hat{\beta}_+\} \geq 0$, we select the estimate closer to the maximum likelihood estimate. That is,

$$\hat{\beta}_T = \begin{cases} \hat{\beta}_-, & \text{if } |\hat{\beta}_- - \hat{\beta}_{MLE}| < |\hat{\beta}_+ - \hat{\beta}_{MLE}|, \\ \hat{\beta}_+, & \text{if } |\hat{\beta}_+ - \hat{\beta}_{MLE}| \leq |\hat{\beta}_- - \hat{\beta}_{MLE}|. \end{cases} \quad (62)$$

Note 9. *Heuristically, the shape parameter α of a distribution is often approximately inversely proportional to the coefficient of variation (CV). Thus, defining $\beta = \alpha^{-1}$, we have that β is approximately proportional to the CV. Therefore, to solve Eq. (60) numerically, we can initialize the iterative algorithm as $\beta_{start} = \widehat{CV}$.* \square

A formal procedure for estimating the parameter vector $(\hat{\beta}_T, \hat{\sigma}_T)$ is summarized in Algorithm 2.

We now calculate $\mathbf{\Sigma}_T$ by using Theorem 1. That is,

$$\begin{aligned}
\sigma_{11}^2 &= \Gamma(1,1)V(1,1) \\
&= \Gamma(1,1) \int_{a_1}^{\bar{b}_1} \int_{a_1}^{\bar{b}_1} K(w,v) H'_1(w) H'_1(v) dv dw \\
&= \beta^2 \Gamma(1,1) \int_{a_1}^{\bar{b}_1} \int_{a_1}^{\bar{b}_1} \frac{K(w,v)}{vw \log(v) \log(w)} dv dw \\
&= \beta^2 \Psi_{111}, \\
\sigma_{12}^2 &= \Gamma(1,2)V(1,2) \\
&= \Gamma(1,2) \int_{a_1}^{\bar{b}_1} \int_{a_2}^{\bar{b}_2} K(w,v) H'_1(w) H'_2(v) dv dw \\
&= 2\beta^2 \Gamma(1,2) \int_{a_1}^{\bar{b}_1} \int_{a_2}^{\bar{b}_2} \frac{K(w,v)}{vw \log(v) \log(w)} (\log(\sigma) - \beta \log(-\log(v))) dv dw \\
&= 2\beta^2 \log(\sigma) \Psi_{121} - 2\beta^3 \Psi_{122}, \tag{63}
\end{aligned}$$

$$\begin{aligned}
\sigma_{22}^2 &= \Gamma(2,2)V(2,2) \\
&= \Gamma(2,2) \int_{a_2}^{\bar{b}_2} \int_{a_2}^{\bar{b}_2} K(w,v) H'_2(w) H'_2(v) dv dw \\
&= 4\beta^2 \Gamma(2,2) \int_{a_2}^{\bar{b}_2} \int_{a_2}^{\bar{b}_2} \frac{K(w,v)}{vw \log(v) \log(w)} (\beta \log(-\log(w)) - \log(\sigma)) (\beta \log(-\log(v)) - \log(\sigma)) dv dw \\
&= 4\beta^2 (\log(\sigma))^2 \Psi_{221} - 8\beta^3 \log(\sigma) \Psi_{222} + 4\beta^4 \Psi_{223}, \tag{64}
\end{aligned}$$

where the double integral terms Ψ_{ijk} , for $1 \leq i, j \leq 2$ and $1 \leq k \leq 3$, do not depend on the parameters to be estimated. The corresponding simplified single-integral expressions, derived using Theorem 1, are provided in Appendix A.

The Jacobian matrix \mathbf{D}_T is found by differentiating the functions g_1 and g_2 from Eq. (55) and then evaluating its derivatives at (T_1, T_2) . That is,

$$d_{11} = \frac{\partial g_1}{\partial \hat{T}_1} \Big|_{(T_1, T_2)} = \frac{-\zeta_r T_1}{\sqrt{\zeta(a_1, \bar{b}_2)}} (T_2 - \zeta_r T_1^2)^{-\frac{1}{2}} + \frac{\kappa_1(a_2, \bar{b}_2) - \kappa_1(a_1, \bar{b}_1)}{\zeta(a_1, \bar{b}_2)}, \tag{65}$$

$$d_{12} = \frac{\partial g_1}{\partial \hat{T}_2} \Big|_{(T_1, T_2)} = \frac{1}{2\sqrt{\zeta(a_1, \bar{b}_2)}} (T_2 - \zeta_r T_1^2)^{-\frac{1}{2}}, \tag{66}$$

$$d_{21} = \frac{\partial g_2}{\partial \hat{T}_1} \Big|_{(T_1, T_2)} = (1 + d_{11} \kappa_1(a_1, \bar{b}_1)) \exp\{T_1 + \beta \kappa_1(a_1, \bar{b}_1)\} = \sigma (1 + d_{11} \kappa_1(a_1, \bar{b}_1)), \tag{67}$$

$$d_{22} = \frac{\partial g_2}{\partial \hat{T}_2} \Big|_{(T_1, T_2)} = d_{12} \kappa_1(a_1, \bar{b}_1) \exp\{T_1 + \beta \kappa_1(a_1, \bar{b}_1)\} = \sigma d_{12} \kappa_1(a_1, \bar{b}_1). \tag{68}$$

Thus, we get

$$\left(\hat{\beta}_T, \hat{\sigma}_T\right) \sim \mathcal{AN}\left((\beta, \sigma), \frac{1}{n} \mathbf{S}_T\right), \quad \text{where } \mathbf{S}_T = \mathbf{D}_T \boldsymbol{\Sigma}_T \mathbf{D}_T'. \quad (69)$$

Again from Bücher and Segers (2018), we can derive

$$\left(\hat{\beta}_{MLE}, \hat{\sigma}_{MLE}\right) \sim \mathcal{AN}\left((\beta, \sigma), \frac{1}{n} \mathbf{S}_{MLE}\right), \quad (70)$$

where

$$\mathbf{S}_{MLE} = \frac{6}{\pi^2} \begin{bmatrix} \beta^2 & (1-\gamma)\sigma\beta^2 \\ (1-\gamma)\sigma\beta^2 & (\sigma\beta)^2 ((\gamma-1)^2 + \pi^2/6) \end{bmatrix} \quad \text{giving } \det(\mathbf{S}_{MLE}) = \frac{6\beta^4\sigma^2}{\pi^2}, \quad (71)$$

and $\gamma := -\Gamma'(1) = 0.57721566490$ is the Euler–Mascheroni constant.

Finally, from Eq. (17) and Eq. (69), we have

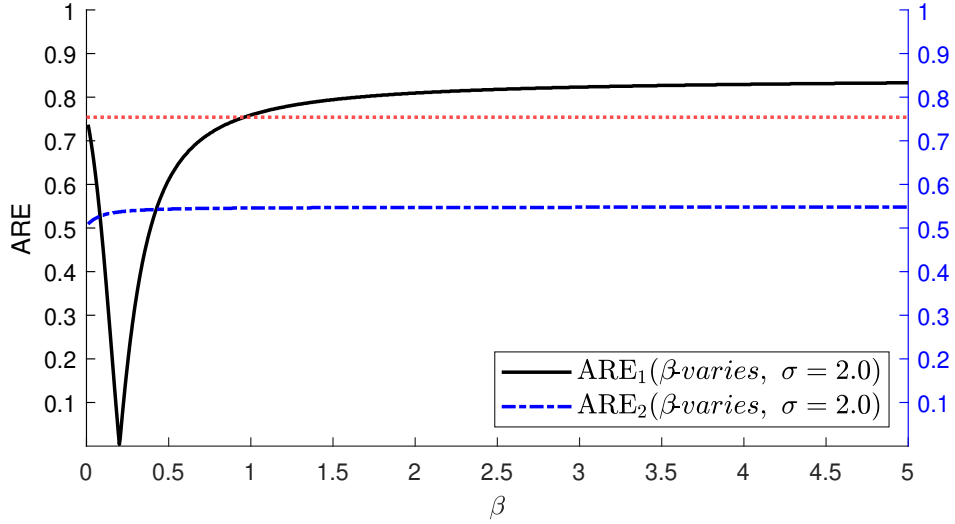
$$ARE\left(\left(\hat{\beta}_T, \hat{\sigma}_T\right), \left(\hat{\beta}_{MLE}, \hat{\sigma}_{MLE}\right)\right) = (\det(\mathbf{S}_{MLE}) / \det(\mathbf{S}_T))^{0.5}. \quad (72)$$

Table 2: From Frechet($\beta, \sigma = 2$), and we vary the tail index β , reciprocal of the shape parameter. A larger β (i.e., a smaller shape parameter α) implies a heavier tail. Inequality used (25).

Proportions		β									
(a_1, b_1)	(a_2, b_2)	0.1	0.2	0.5	1	2	5	10	15	25	
(0.02, 0.02)	(0.02, 0.02)	0.771	0.771	0.771	0.771	0.771	0.771	0.771	0.771	0.771	
(0.02, 0.02)	(0.00, 0.04)	0.259	0.633	0.786	0.815	0.827	0.833	0.834	0.835	0.835	
(0.05, 0.05)	(0.05, 0.05)	0.754	0.754	0.754	0.754	0.754	0.754	0.754	0.754	0.754	
(0.05, 0.05)	(0.00, 0.10)	0.458	0.004	0.610	0.759	0.809	0.833	0.840	0.842	0.844	
(0.10, 0.10)	(0.10, 0.10)	0.693	0.693	0.693	0.693	0.693	0.693	0.693	0.693	0.693	
(0.10, 0.10)	(0.00, 0.20)	0.760	0.624	0.036	0.560	0.736	0.802	0.819	0.824	0.828	
(0.15, 0.15)	(0.15, 0.15)	0.623	0.623	0.623	0.623	0.623	0.623	0.623	0.623	0.623	
(0.15, 0.15)	(0.00, 0.30)	0.812	0.762	0.439	0.296	0.674	0.786	0.810	0.817	0.822	

Like in Section 3.1, several key findings emerge from Table 2 and Figure 3. In Figure 3, the horizontal red dotted line represents the ARE value obtained using identical trimming proportions for both moments, i.e., $(a_1, b_1) = (a_2, b_2) = (0.05, 0.05)$.

Unlike the location-scale model, where the distribution may be symmetric about the origin, the Fréchet model considered here is strictly positive. Therefore, trimming inequalities (25) and (31) lead to different subsets of data being excluded for different moments. As shown in the top panel of Figure 3, and under trimming inequality (25), the ARE values remain higher than those from equal trimming when $T_2 - \zeta_r T_1^2 \gg 0$. For example, the ARE drops sharply at approximately $\beta = 0.2$ and $\sigma = 2$, where $T_2 - \zeta_r T_1^2 = 5.2052 \times 10^{-7}$.



$$\begin{aligned}
 ARE_1(\beta\text{-varies, } \sigma = 2) &= ARE(\beta\text{-varies, } \sigma = 2, (a_1, b_1) = (0.05, 0.05), (a_2, b_2) = (0.00, 0.10)) \\
 ARE_2(\beta\text{-varies, } \sigma = 2) &= ARE(\beta\text{-varies, } \sigma = 2, (a_1, b_1) = (0.05, 0.05), (a_2, b_2) = (0.10, 0.00)) \\
 ARE_1(\beta = 2, \sigma\text{-varies}) &= ARE(\beta = 2, \sigma\text{-varies}, (a_1, b_1) = (0.05, 0.05), (a_2, b_2) = (0.00, 0.10)) \\
 ARE_2(\beta = 2, \sigma\text{-varies}) &= ARE(\beta = 2, \sigma\text{-varies}, (a_1, b_1) = (0.05, 0.05), (a_2, b_2) = (0.10, 0.00))
 \end{aligned}$$

Figure 3: Fréchet ARE curves under trimming inequalities (25) or (31).

For $\beta \geq 1$ and $\sigma = 1$, the ARE values under trimming inequality (25) exceed those under equal trimming, as seen by the black curve lying above the red dotted line. This indicates that for heavier-tailed Fréchet distributions, using distinct trimming proportions for each moment can yield higher efficiency than applying the same trimming to both.

In contrast, the ARE values under trimming inequality (31) remain consistently flat. This is because

the scenario $T_2 - \zeta_r T_1^2 \rightarrow 0^+$ rarely occurs under this configuration.

The interpretation of the bottom panel in Figure 3 is similar. The ARE curve corresponding to trimming inequality (25) decreases with increasing σ until $T_2 - \zeta_r T_1^2 \rightarrow 0^+$, after which it begins to rise again. The ARE curve under trimming inequality (31) remains nearly constant throughout.

4 Simulation Study

This section complements the theoretical results developed in previous sections with simulation studies. The primary objectives are to determine the sample size required for the estimators to become effectively unbiased (given their asymptotic unbiasedness), validate their asymptotic normality, and evaluate their finite-sample relative efficiencies (REs) in relation to their corresponding asymptotic relative efficiencies (AREs). To compute the RE of MTM estimators, we use the MLE as the benchmark. Accordingly, the definition of ARE in Eq. (17) is adapted for finite-sample performance as follows:

$$RE(\text{MTM, MLE}) = \frac{\text{asymptotic variance of MLE estimator}}{\text{small-sample variance of a competing MTM estimator}}, \quad (73)$$

where the numerator is defined in Eq. (17), and the denominator is expressed as:

$$\left(\det \begin{bmatrix} E[(\hat{\theta} - \theta)^2] & E[(\hat{\theta} - \theta)(\hat{\sigma} - \sigma)] \\ E[(\hat{\theta} - \theta)(\hat{\sigma} - \sigma)] & E[(\hat{\sigma} - \sigma)^2] \end{bmatrix} \right)^{1/2}.$$

From a specified distribution F , we generate 10,000 samples of a given length n using Monte Carlo simulations. For each sample, we estimate the parameters of F using various T -estimators under trimming inequality (25) or (31), and compute the sample mean and relative efficiency (RE) from 10,000 replicates. This procedure is repeated 10 times, and the averages of the resulting 10 means and 10 REs, along with their standard deviations, are reported.

We start the simulation study with the normal distribution $N(\theta = 0.1, \sigma^2 = 5^2)$, using the following specifications.

- Sample size: $n = 100, 500, 1000$.
- Estimators of θ and σ :

- MLE,
- MTM using trimming proportions specified by either inequality (25) or (31)

Table 3: Normal model with parameters $\theta = 0.1$ and $\sigma = 5$.

Estimator		$n = 100$		$n = 500$		$n = 1000$		$n \rightarrow \infty$	
(a_1, b_1)	(a_2, b_2)	$\hat{\theta}/\theta$	$\hat{\sigma}/\sigma$	$\hat{\theta}/\theta$	$\hat{\sigma}/\sigma$	$\hat{\theta}/\theta$	$\hat{\sigma}/\sigma$	$\hat{\theta}/\theta$	$\hat{\sigma}/\sigma$
Mean values of $\hat{\theta}/\theta$ and $\hat{\sigma}/\sigma$.									
MLE		0.98	0.99	1.01	1.00	1.00	1.00	1	1
(0.00, 0.00)	(0.00, 0.00)	0.98	0.99	1.01	1.00	1.00	1.00	1	1
(0.00, 0.05)	(0.00, 0.05)	1.10	1.00	1.01	1.00	1.00	1.00	1	1
(0.00, 0.10)	(0.00, 0.10)	1.10	1.00	1.02	1.00	1.01	1.00	1	1
With strict trimming inequality (25).									
(0.10, 0.00)	(0.05, 0.05)	0.84	1.00	0.98	1.00	0.98	1.00	1	1
(0.05, 0.05)	(0.00, 0.10)	1.00	0.99	1.00	1.00	1.00	1.00	1	1
(0.10, 0.10)	(0.00, 0.20)	1.01	0.99	1.00	1.00	1.00	1.00	1	1
(0.15, 0.15)	(0.00, 0.30)	0.97	0.99	1.01	1.00	1.01	1.00	1	1
With strict trimming inequality (31).									
(0.00, 0.10)	(0.05, 0.05)	1.07	1.00	1.02	1.00	1.01	1.00	1	1
(0.05, 0.05)	(0.10, 0.00)	1.00	0.99	0.99	1.00	1.00	1.00	1	1
(0.10, 0.10)	(0.20, 0.00)	0.99	0.99	1.00	1.00	1.00	1.00	1	1
(0.15, 0.15)	(0.30, 0.00)	1.00	0.99	1.00	1.00	1.00	1.00	1	1
(0.25, 0.50)	(0.50, 0.25)	1.03	1.00	1.00	1.00	1.00	1.00	1	1
Finite-sample efficiencies (RE) of MTMs relative to MLEs.									
MLE		0.999		0.996		0.994		1	
(0.00, 0.00)	(0.00, 0.00)	0.999		0.996		0.994		1	
(0.00, 0.05)	(0.00, 0.05)	0.930		0.934		0.929		0.932	
(0.00, 0.10)	(0.00, 0.10)	0.877		0.876		0.876		0.872	
With strict trimming inequality (25).									
(0.10, 0.00)	(0.05, 0.05)	0.874		0.870		0.872		0.872	
(0.05, 0.05)	(0.00, 0.10)	0.884		0.882		0.881		0.883	
(0.10, 0.10)	(0.00, 0.20)	0.808		0.801		0.805		0.805	
(0.15, 0.15)	(0.00, 0.30)	0.753		0.748		0.752		0.752	
With strict trimming inequality (31).									
(0.00, 0.10)	(0.05, 0.05)	0.874		0.880		0.872		0.876	
(0.05, 0.05)	(0.10, 0.00)	0.888		0.889		0.881		0.884	
(0.10, 0.10)	(0.20, 0.00)	0.807		0.805		0.810		0.807	
(0.15, 0.15)	(0.30, 0.00)	0.758		0.754		0.760		0.754	
(0.25, 0.50)	(0.50, 0.25)	0.493		0.491		0.488		0.491	

The simulation results are summarized in Table 3. All estimators in the normal case accurately recover both the location parameter θ and the scale parameter σ , becoming nearly unbiased for sample sizes as small as $n = 100$. The relative bias of θ estimators under trimming inequality (25) is generally negative, while that under inequality (31) tends to be positive. This pattern aligns with

the explanation in Note 3: when $\theta = 0.1$, trimming under inequality (25) is more likely to remove the same observations from both moments, preserving balance. In contrast, under inequality (31), where $\bar{b}_1 \leq \bar{b}_2$, fewer large values are excluded from the second moment, potentially inflating the location estimate. The finite relative efficiencies (FREs) also approach their asymptotic limits, with some converging from above.

Table 4: Fréchet model with parameters $\beta = 5$ and $\sigma = 2$.

Estimator		$n = 100$		$n = 500$		$n = 1000$		$n \rightarrow \infty$	
(a_1, b_1)	(a_2, b_2)	$\hat{\beta}/\beta$	$\hat{\sigma}/\sigma$	$\hat{\beta}/\beta$	$\hat{\sigma}/\sigma$	$\hat{\beta}/\beta$	$\hat{\sigma}/\sigma$	$\hat{\beta}/\beta$	$\hat{\sigma}/\sigma$
Mean values of $\hat{\theta}/\theta$ and $\hat{\sigma}/\sigma$.									
MLE		0.99	1.17	1.00	1.03	1.00	1.01	1	1
(0.00, 0.00)	(0.00, 0.00)	0.99	1.19	1.00	1.03	1.00	1.02	1	1
(0.00, 0.05)	(0.00, 0.05)	1.00	1.18	1.00	1.03	1.00	1.02	1	1
(0.00, 0.10)	(0.00, 0.10)	1.00	1.19	1.00	1.03	1.00	1.02	1	1
With strict trimming inequality (25).									
(0.10, 0.00)	(0.05, 0.05)	1.01	1.15	1.00	1.03	1.00	1.01	1	1
(0.05, 0.05)	(0.00, 0.10)	1.00	1.17	1.00	1.03	1.00	1.02	1	1
(0.10, 0.10)	(0.00, 0.20)	1.00	1.18	1.00	1.03	1.00	1.02	1	1
(0.15, 0.15)	(0.00, 0.30)	1.00	1.18	1.00	1.03	1.00	1.02	1	1
With strict trimming inequality (31).									
(0.00, 0.10)	(0.05, 0.05)	1.00	1.19	1.00	1.03	1.00	1.02	1	1
(0.05, 0.05)	(0.10, 0.00)	0.99	1.26	1.00	1.05	1.00	1.02	1	1
(0.10, 0.10)	(0.20, 0.00)	0.99	1.27	1.00	1.05	1.00	1.03	1	1
(0.15, 0.15)	(0.30, 0.00)	0.99	1.29	1.00	1.05	1.00	1.03	1	1
(0.25, 0.50)	(0.50, 0.25)	1.00	1.23	1.00	1.04	1.00	1.02	1	1
Finite-sample efficiencies (RE) of MTMs relative to MLEs.									
MLE		0.729		0.934		0.971		1	
(0.00, 0.00)	(0.00, 0.00)	0.509		0.651		0.671		0.690	
(0.00, 0.05)	(0.00, 0.05)	0.626		0.803		0.831		0.856	
(0.00, 0.10)	(0.00, 0.10)	0.629		0.817		0.849		0.875	
With strict trimming inequality (25).									
(0.10, 0.00)	(0.05, 0.05)	0.448		0.588		0.606		0.627	
(0.05, 0.05)	(0.00, 0.10)	0.614		0.784		0.809		0.833	
(0.10, 0.10)	(0.00, 0.20)	0.583		0.753		0.773		0.802	
(0.15, 0.15)	(0.00, 0.30)	0.549		0.737		0.759		0.786	
With strict trimming inequality (31).									
(0.00, 0.10)	(0.05, 0.05)	0.563		0.723		0.753		0.774	
(0.05, 0.05)	(0.10, 0.00)	0.378		0.512		0.526		0.548	
(0.10, 0.10)	(0.20, 0.00)	0.348		0.467		0.487		0.509	
(0.15, 0.15)	(0.30, 0.00)	0.317		0.448		0.470		0.489	
(0.25, 0.50)	(0.50, 0.25)	0.308		0.424		0.436		0.457	

Similarly, we continue the simulation study with the Fréchet distribution $F(\beta = 5, \sigma = 2)$, using the following specifications.

- Sample size: $n = 100, 500, 1000$.
- Estimators of θ and σ :
 - MLE,
 - MTM using trimming proportions specified by either inequality (25) or (31)

The simulation results are summarized in Table 4. As in the normal case, all estimators in the Fréchet model accurately recover both parameters β and σ as the sample size increases and relative bias decreases. The estimator for β becomes nearly unbiased for sample sizes as small as $n = 100$. However, the relative bias of the σ estimators is generally lower under trimming inequality (25) compared to inequality (31), which is expected. For instance, under inequality (25) with $(a_1, b_1) = (0.05, 0.05)$ and $(a_2, b_2) = (0.00, 0.10)$, a greater proportion of large observations are excluded from the second moment calculation. In contrast, under inequality (31) with the same (a_1, b_1) but $(a_2, b_2) = (0.10, 0.00)$, the second moment retains all larger values due to the absence of right-side trimming, resulting in higher bias for the scale parameter σ . The finite relative efficiencies (FREs) also converge toward their asymptotic counterparts, though at a slower rate, with some approaching from above.

5 Real Data Analysis

In this section, we apply both the MTM and MLE approaches to analyze the normalized damage amounts from the 30 most damaging hurricanes in the United States between 1925 and 1995, as reported by [Pielke and Landsea \(1998\)](#). This dataset has previously been examined using the same trimming proportions for all moments by [Brazauskas *et al.* \(2009\)](#), and using the same winsorizing proportions for all moments by [Zhao *et al.* \(2018\)](#). The damage figures were normalized to 1995 dollars, accounting for inflation, changes in personal property values, and coastal county population growth. Our objective is to assess how initial assumptions and parameter estimation methods influence model fit.

Both lognormal and Fréchet models provide a good fit to the hurricane damage data, with maximum likelihood estimates summarized in the MLE row of Table 5. The corresponding p -values are 0.9678 and 0.7611, respectively, and the fitted CDFs are shown alongside the empirical CDF in Figure 4. At

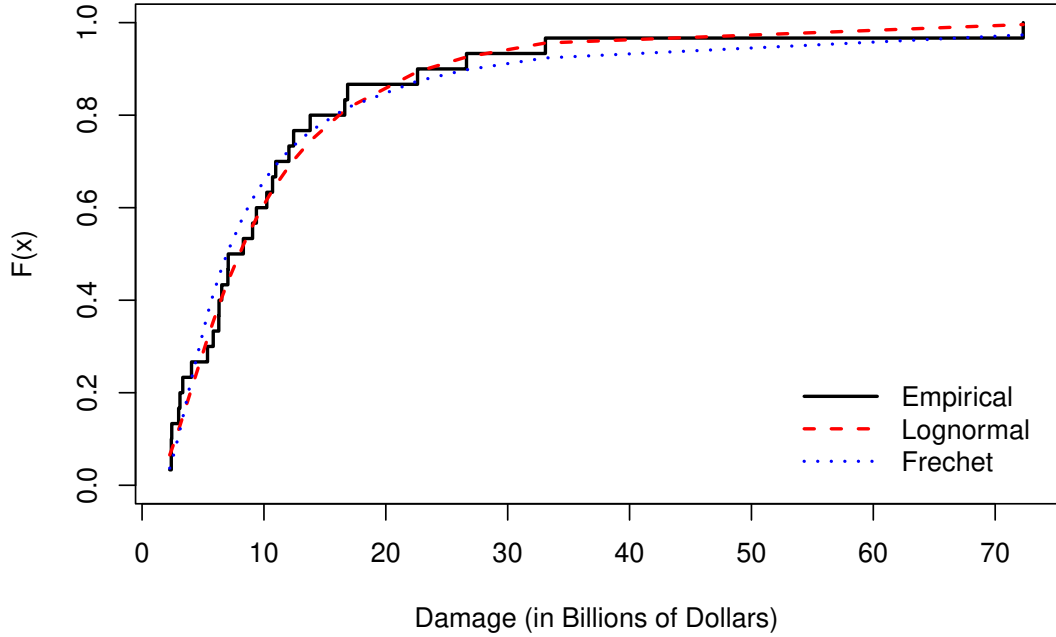


Figure 4: Empirical cumulative distribution function (CDF) of the hurricane damage data overlaid with fitted CDFs from the lognormal and Fréchet models, illustrating the diagnostic fit performance of each model.

the 5% significance level, neither model is rejected, indicating that both are plausible for modeling the data.

To further evaluate the robustness of the proposed flexible trimming approach, we follow [Brazauskas *et al.* \(2009\)](#) and introduce a mild data modification by replacing the largest observation, 72.303, with 723.03. The resulting parameter estimates and goodness-of-fit (GOF) measures, using different trimming proportions defined by inequalities (25) and (31), are presented in Table 5 for both the original and modified datasets. The goodness-of-fit is assessed using the mean absolute deviation

$$\text{FIT} := \frac{1}{30} \sum_{j=1}^{30} \left| \log \left(\hat{F}^{-1} \left(\frac{j-0.5}{30} \right) \right) - \log (X_{j:30}) \right|,$$

between the log-fitted and log-observed data ([Brazauskas *et al.*, 2009](#)), along with AIC and BIC.

Several conclusions emerge from this analysis. First, the goodness-of-fit (GOF) statistics for most robust MTM estimators remain stable under data modification, provided the trimming proportions are nonzero. In contrast, the MLE fit changes substantially. The GOF values are notably higher

Table 5: Parameter estimates and goodness-of-fit measures for the lognormal and Fréchet models fitted to the original and modified hurricane loss data.

Est.	Proportion		Lognormal Model					Fréchet Model				
	(a_1, b_1)	(a_2, b_2)	$\hat{\theta}$	$\hat{\sigma}$	FIT	AIC	BIC	$\hat{\beta}$	$\hat{\sigma}^*$	FIT	AIC	BIC
Original Data												
MLE	—		22.80	0.83	0.1036	1446	1449	0.72	5.35	0.1277	1446	1448
T_1	(0, 0)	(0, 0)	22.80	0.83	0.1036	1446	1449	0.65	5.48	0.1168	1446	1449
T_2	(0, 1/30)	(0, 1/30)	22.79	0.80	0.1069	1446	1449	0.69	5.44	0.1199	1446	1449
T_3	(1/30, 1/30)	(1/30, 1/30)	22.77	0.85	0.1013	1446	1449	0.70	5.39	0.1222	1446	1449
T_4	(7/30, 7/30)	(7/30, 7/30)	22.78	0.77	0.1133	1447	1449	0.66	6.03	0.1219	1448	1451
T_5	(0, 0)	(0, 1/30)	22.80	2.91	1.6402	1494	1497	0.54	5.83	0.1719	1454	1457
T_6	(1/30, 1/30)	(0, 2/30)	22.77	7.30	5.1024	1558	1561	0.58	5.73	0.1443	1450	1453
T_7	(1/30, 1/30)	(2/30, 0)	22.77	0.88	0.1016	1446	1449	0.63	5.60	0.1186	1447	1450
T_8	(0, 3/30)	(0, 0)	22.80	0.90	0.1107	1447	1449	0.60	5.64	0.1298	1448	1451
T_9	(4/30, 5/30)	(5/30, 2/30)	22.76	0.87	0.1026	1446	1449	0.66	5.73	0.1114	1447	1449
T_{10}	(7/30, 15/30)	(15/30, 7/30)	22.78	0.78	0.1108	1447	1449	0.67	6.00	0.1250	1447	1450
Modified Data												
MLE	—		22.88	1.10	0.2932	1467	1470	0.77	5.47	0.1896	1456	1459
T_1	(0, 0)	(0, 0)	22.88	1.10	0.2932	1467	1470	0.86	5.26	0.2121	1457	1460
T_2	(0, 1/30)	(0, 1/30)	22.79	0.80	0.1838	1475	1478	0.69	5.44	0.1813	1457	1460
T_3	(1/30, 1/30)	(1/30, 1/30)	22.77	0.85	0.1781	1472	1475	0.70	5.39	0.1818	1457	1460
T_4	(7/30, 7/30)	(7/30, 7/30)	22.78	0.77	0.1900	1478	1480	0.66	6.03	0.1846	1459	1462
T_5	(0, 0)	(0, 1/30)	22.88	3.86	2.3122	1515	1518	1.50	3.62	0.7212	1476	1479
T_6	(1/30, 1/30)	(0, 2/30)	22.77	7.30	5.0255	1552	1554	0.58	5.73	0.2211	1463	1466
T_7	(1/30, 1/30)	(2/30, 0)	22.77	1.41	0.4813	1471	1474	1.00	4.61	0.3133	1461	1464
T_8	(0, 3/30)	(0, 0)	22.87	1.27	0.3887	1468	1471	0.85	5.27	0.2112	1457	1460
T_9	(4/30, 5/30)	(5/30, 2/30)	22.76	0.87	0.1793	1472	1474	0.66	5.73	0.1766	1458	1461
T_{10}	(7/30, 15/30)	(15/30, 7/30)	22.78	0.78	0.1876	1477	1479	0.67	6.00	0.1844	1459	1461

NOTE: Est. stands for Estimators. Fréchet estimated scale parameter $\hat{\sigma} = \hat{\sigma}^* \times 10^9$.

for T_5 and T_6 under both models. This may be attributed, as discussed in Note 3, to the strictly positive support of the sample data and the fitted lognormal model, suggesting that trimming based on inequality (31) is more appropriate than inequality (25), which assumes approximate symmetry about the origin.

Second, the increase in GOF is more pronounced for T_7 than for MLE when comparing original and modified data. This is expected, as T_7 involves no right-tail trimming for the second moment, allowing the inflated maximum value to influence the fit.

Third, under T_2 , T_3 , T_4 , T_9 , and T_{10} , parameter estimates for both models remain unchanged between original and modified data, reflecting the robustness of MTM. Notably, T_{10} —which uses disjoint middle portions of the data for the two moments—produces low GOF values under the Fréchet model, even with data contamination.

Fourth, the Fréchet tail index estimate $\hat{\beta}$ is consistently below one, except for T_5 and T_7 under the modified data, suggesting a lighter right tail in the sample. This supports the higher p -value

observed for the lognormal fit compared to the Fréchet fit. Overall, the lognormal model appears more suitable for the original data, while the robust Fréchet model is better suited when the data contain a large outlier.

6 Conclusion

This paper introduced a general and flexible framework for robust parametric estimation based on trimmed L -moments (MTM), allowing distinct trimming proportions for different moments. The proposed approach extends traditional trimmed moment methods by enabling asymmetric and moment-specific trimming strategies, which improve robustness against outliers and model misspecification without sacrificing computational tractability. Estimators derived under this framework maintain closed-form expressions and avoid iterative optimization, making them suitable for large-scale data analysis. We derived their asymptotic properties under the general theory of L -statistics and provided analytical variance expressions to support comparative efficiency analysis.

Simulation studies across various scenarios demonstrate that the proposed estimators offer strong finite-sample performance and effectively balance robustness and efficiency. The flexibility to assign distinct trimming proportions to different moments enhances adaptability to the data structure and contamination patterns. This advantage is especially evident in asymmetric or heavy-tailed settings, where the general MTM consistently outperforms classical and symmetric-trimming methods in terms of bias and mean squared error.

The practical utility of the proposed methodology was further validated using a real-world dataset of the 30 most damaging hurricanes in the United States. Both lognormal and Fréchet models were fitted using MLE and several MTM variants. The results confirmed that MLE is highly sensitive to data perturbations, while MTM estimates remained stable and interpretable. When the largest loss was inflated by a factor of 10, the properly designed MTM estimators remained consistent, whereas the MLE fit deteriorated considerably, especially under the Fréchet model. Moreover, goodness-of-fit metrics (e.g., AIC, BIC, and empirical quantile deviation) reinforced the robustness and adaptability of the MTM framework in both original and modified datasets.

Overall, the proposed general MTM approach offers a simple yet powerful extension of L -estimation techniques, making it a valuable tool for robust inference in the presence of contamination or heavy tails. Future work may include extending the framework to mixture models, multivariate

distributions, incorporating covariate information, or applying the methodology to other domains such as environmental risk, finance, and reliability analysis.

References

Brazauskas, V., Jones, B.L., and Zitikis, R. (2009). Robust fitting of claim severity distributions and the method of trimmed moments. *Journal of Statistical Planning and Inference*, **139**(6), 2028–2043.

Brazauskas, V. and Kleefeld, A. (2009). Robust and efficient fitting of the generalized Pareto distribution with actuarial applications in view. *Insurance: Mathematics & Economics*, **45**(3), 424–435.

Bücher, A. and Segers, J. (2018). Maximum likelihood estimation for the Fréchet distribution based on block maxima extracted from a time series. *Bernoulli*, **24**(2), 1427–1462.

Chernoff, H., Gastwirth, J.L., and Johns, Jr., M.V. (1967). Asymptotic distribution of linear combinations of functions of order statistics with applications to estimation. *Annals of Mathematical Statistics*, **38**(1), 52–72.

Gatti, S. and Wüthrich, M.V. (2025). Modeling lower-truncated and right-censored insurance claims with an extension of the MBBEFD class. *European Actuarial Journal*, **15**(1), 199–240.

Hampel, F.R., Ronchetti, E.M., Rousseeuw, P.J., and Stahel, W.A. (1986). *Robust Statistics: The Approach Based on Influence Functions*. John Wiley & Sons, Inc., New York.

Hao, S., Yang, J., and Li, W. (2014). A robust bootstrap confidence interval for the two-parameter Weibull distribution based on the method of trimmed moments. *2014 Prognostics and System Health Management Conference (PHM-2014 Hunan)*, pages 478–481.

Huber, P.J. and Ronchetti, E.M. (2009). *Robust Statistics*. Second edition. John Wiley & Sons, Inc., Hoboken, NJ.

Kim, J.H.T. and Jeon, Y. (2013). Credibility theory based on trimming. *Insurance: Mathematics & Economics*, **53**(1), 36–47.

Kleefeld, A. and Brazauskas, V. (2012). A statistical application of the quantile mechanics approach: MTM estimators for the parameters of t and gamma distributions. *European Journal of Applied Mathematics*, **23**(5), 593–610.

Nawa, V. and Nadarajah, S. (2025). Logarithmic method of moments estimators for the Fréchet distribution. *Journal of Computational and Applied Mathematics*, **457**, Paper No. 116293, 9.

Opdyke, J. and Cavallo, A. (2012). Estimating operational risk capital: the challenges of truncation, the hazards of MLE, and the promise of robust statistics. *Journal of Operational Risk*, **7**(3), 3–90.

Pielke, Jr., R.A. and Landsea, C.W. (1998). Normalized hurricane damages in the United States: 1925–1995. *Weather and Forecasting*, **13**, 621–631.

Poudyal, C. (2021). Robust estimation of loss models for lognormal insurance payment severity data. *ASTIN Bulletin – The Journal of the International Actuarial Association*, **51**(2), 475–507.

Poudyal, C. (2025). On the asymptotic normality of trimmed and winsorized L-statistics. *Communications in Statistics – Theory and Methods*, **54**(10), 3114–3133.

Poudyal, C. and Brazauskas, V. (2023). Finite-sample performance of the T - and W -estimators for the Pareto tail index under data truncation and censoring. *Journal of Statistical Computation and Simulation*, **93**(10), 1601–1621.

Schott, J.R. (2017). *Matrix Analysis for Statistics*. Wiley Series in Probability and Statistics, third edition. John Wiley & Sons, Inc., Hoboken, NJ.

Serfling, R. (2002). Efficient and robust fitting of lognormal distributions. *North American Actuarial Journal*, **6**(4), 95–109.

Serfling, R.J. (1980). *Approximation Theorems of Mathematical Statistics*. John Wiley & Sons, New York.

Shaked, M. and Shanthikumar, J.G. (2007). *Stochastic Orders*. Springer, New York.

Tukey, J.W. (1960). A survey of sampling from contaminated distributions. *Contributions to Probability and Statistics*, pages 448–485. Stanford University Press, Stanford, CA.

Zhao, Q., Brazauskas, V., and Ghorai, J. (2018). Robust and efficient fitting of severity models and the method of Winsorized moments. *ASTIN Bulletin – The Journal of the International Actuarial Association*, **48**(1), 275–309.

Appendix A: Proofs

PROOF OF PROPOSITION 1: Define

$$U_\tau \sim \text{Uniform}(a_\tau, \bar{b}_\tau) \quad \text{and} \quad W_\tau := F_0^{-1}(U_\tau), \quad \tau \in \{i, j\}.$$

Then, for any positive integer k , it follows that

$$c_k(a_\tau, \bar{b}_\tau) = \mathbb{E}[W_\tau^k].$$

(i) Thus, we get

$$\begin{aligned} \eta(a_i, \bar{b}_j) &= c_1^2(a_i, \bar{b}_i) - 2c_1(a_i, \bar{b}_i)c_1(a_j, \bar{b}_j) + c_2(a_j, \bar{b}_j) \\ &= (\mathbb{E}[W_i])^2 - 2\mathbb{E}[W_i]\mathbb{E}[W_j] + \mathbb{E}[W_j^2] \\ &= (\mathbb{E}[W_i] - \mathbb{E}[W_j])^2 + \mathbb{E}[W_j^2] - (\mathbb{E}[W_j])^2 \\ &= (\mathbb{E}[W_i] - \mathbb{E}[W_j])^2 + \text{Var}[W_j]. \end{aligned} \quad (74)$$

Since W_j is a non-degenerate random variable giving $\text{Var}[W_j] > 0$ and $(\mathbb{E}[W_i] - \mathbb{E}[W_j])^2 \geq 0$, Eq. (74) takes the form

$$\eta(a_i, \bar{b}_j) = (\mathbb{E}[W_i] - \mathbb{E}[W_j])^2 + \text{Var}[W_j] > 0.$$

(ii) With the given inequality (8), U_j is smaller than U_i in stochastic order (see, e.g., [Shaked and Shanthikumar, 2007](#), Ch 1), i.e., $U_j \leq_{\text{st}} U_i$. Being a quantile function of the standard location-scale family of distributions, F_0^{-1} is strictly increasing, then again it follows that ([Shaked and Shanthikumar, 2007](#), Theorem 1.A.3), $W_j \leq_{\text{st}} W_i$. For odd positive integer k , $g(x) = x^k$ is strictly an increasing function, giving $W_j^k \leq_{\text{st}} W_i^k$. Thus,

$$\mathbb{E}[W_j^k] \leq \mathbb{E}[W_i^k], \quad \text{i.e.,} \quad c_k(a_j, \bar{b}_j) \leq c_k(a_i, \bar{b}_i). \quad (75)$$

(iii) From (i), it immediately follows that $0 < \eta_r$. Further, we know that $\eta(a_j, \bar{b}_j) = \text{Var}[W_j]$. Thus from Eq. (74), it follows that

$$\eta_r = \frac{\eta(a_j, \bar{b}_j)}{\eta(a_i, \bar{b}_j)} = \frac{\text{Var}[W_j]}{(\mathbb{E}[W_i] - \mathbb{E}[W_j])^2 + \text{Var}[W_j]} \leq 1.$$

(iv) We have

$$\begin{aligned} &c_2(a_j, \bar{b}_j) \geq \eta_r c_1^2(a_i, \bar{b}_i) \\ \iff &c_2(a_j, \bar{b}_j) \eta(a_i, \bar{b}_j) \geq c_1^2(a_i, \bar{b}_i) \eta(a_j, \bar{b}_j) \\ \iff &c_2(a_j, \bar{b}_j) (c_1^2(a_i, \bar{b}_i) - 2c_1(a_i, \bar{b}_i)c_1(a_j, \bar{b}_j) + c_2(a_j, \bar{b}_j)) \\ &\geq c_1^2(a_i, \bar{b}_i) (c_2(a_j, \bar{b}_j) - c_1^2(a_j, \bar{b}_j)) \\ \iff &c_2^2(a_j, \bar{b}_j) - 2c_1(a_i, \bar{b}_i)c_1(a_j, \bar{b}_j)c_2(a_j, \bar{b}_j) + c_1^2(a_i, \bar{b}_i)c_1^2(a_j, \bar{b}_j) \\ \iff &(c_2(a_j, \bar{b}_j) - c_1(a_i, \bar{b}_i)c_1(a_j, \bar{b}_j))^2 \geq 0, \end{aligned}$$

a valid inequality as desired.

(v) For $\theta = 0$ and $\sigma = 1$, this converts to the inequality given in (iv). Further, if θ is positive, then this inequality again follows immediately from (iv). But in general, it follows that

$$\begin{aligned} & \eta(a_i, \bar{b}_j) T_2 - \eta(a_j, \bar{b}_j) T_1^2 \\ &= \left(c_2(a_j, \bar{b}_j) \sigma - c_1(a_i, \bar{b}_i) c_1(a_j, \bar{b}_j) \sigma + c_1(a_j, \bar{b}_j) \theta - c_1(a_i, \bar{b}_i) \theta \right)^2 \\ &= \left(\sigma(c_2(a_j, \bar{b}_j) - c_1(a_i, \bar{b}_i) c_1(a_j, \bar{b}_j)) + \theta(c_1(a_j, \bar{b}_j) - c_1(a_i, \bar{b}_i)) \right)^2 \\ &\geq 0. \end{aligned}$$

Thus,

$$\eta(a_i, \bar{b}_j) T_2 - \eta(a_j, \bar{b}_j) T_1^2 \geq 0 \implies T_2 - \eta_r T_1^2 \geq 0, \quad (76)$$

as $\eta(a_i, \bar{b}_j) > 0$ from (i). \square

PROOF OF COROLLARY 2: (i), (iii), (iv), and (v) follow by similar arguments as in Proposition 1. Note that $\log(-\log(u))$ is a decreasing function of $u \in (0, 1)$, which establishes (ii). \square

Appendix B: Asymptotic Covariance Matrix Entries

Here we summarize the simplified single-integral expressions for the asymptotic variance-covariance entries corresponding to the parametric examples discussed in Section 3.

By applying Theorem 1 under the trimming inequality (25), the definitions of the notations Λ_{ijk} , for $1 \leq i, j \leq 2$ and $1 \leq k \leq 3$, as used in Eqs. (38)–(40), are given below:

$$\begin{aligned} \Lambda_{111} &= \Gamma(1, 1) \int_{a_1}^{\bar{b}_1} \int_{a_1}^{\bar{b}_1} K(w, v) dF_0^{-1}(v) dF_0^{-1}(w) dv dw \\ &= \Gamma(1, 1) \left\{ a_1 \bar{a}_1 [F_0^{-1}(a_1)]^2 + b_1 \bar{b}_1 [F_0^{-1}(\bar{b}_1)]^2 - 2 a_1 b_1 F_0^{-1}(a_1) F_0^{-1}(\bar{b}_1) \right. \\ &\quad - 2(1 - a_1 - b_1) [a_1 F_0^{-1}(a_1) + b_1 F_0^{-1}(\bar{b}_1)] c_1(a_1, \bar{b}_1) \\ &\quad \left. - [\Gamma(1, 1)]^{-1} c_1^2(a_1, \bar{b}_1) + (1 - a_1 - b_1) c_2(a_1, \bar{b}_1) \right\}, \\ \Lambda_{121} &= \Gamma(1, 2) \int_{a_1}^{\bar{b}_1} \int_{a_2}^{\bar{b}_2} K(w, v) dF_0^{-1}(v) dF_0^{-1}(w) dv dw \\ &= \Gamma(1, 2) \left\{ a_2 \bar{a}_1 F_0^{-1}(a_1) F_0^{-1}(a_2) + b_1 \bar{b}_2 F_0^{-1}(\bar{b}_1) F_0^{-1}(\bar{b}_2) \right. \\ &\quad - a_1 b_2 F_0^{-1}(a_1) F_0^{-1}(\bar{b}_2) - a_2 b_1 F_0^{-1}(a_2) F_0^{-1}(\bar{b}_1) \\ &\quad - (1 - a_1 - b_2) [2a_1 F_0^{-1}(a_1) + b_1 F_0^{-1}(\bar{b}_1) + b_2 F_0^{-1}(\bar{b}_2)] c_1(a_1, \bar{b}_2) \\ &\quad - (1 - a_1 - b_2)^2 c_1^2(a_1, \bar{b}_2) + (1 - a_1 - b_2) c_2(a_1, \bar{b}_2) \\ &\quad + (1 - a_1 - b_1) [a_1 F_0^{-1}(a_1) - a_2 F_0^{-1}(a_2)] c_1(a_1, \bar{b}_1) \\ &\quad + (a_1 - a_2) \left\{ \bar{a}_1 F_0^{-1}(a_1) - b_1 F_0^{-1}(\bar{b}_1) - (1 - a_1 - b_1) c_1(a_1, \bar{b}_1) \right\} c_1(a_2, a_1) \\ &\quad \left. + (b_2 - b_1) \left\{ \bar{b}_2 F_0^{-1}(\bar{b}_2) - a_1 F_0^{-1}(a_1) - (1 - a_1 - b_2) c_1(a_1, \bar{b}_2) \right\} c_1(\bar{b}_2, \bar{b}_1) \right\}, \end{aligned}$$

$$\begin{aligned}
\Lambda_{122} &= \Gamma(1, 2) \int_{a_1}^{\bar{b}_1} \int_{a_2}^{\bar{b}_2} K(w, v) F_0^{-1}(v) dF_0^{-1}(v) dF_0^{-1}(w) dv dw \\
&= \frac{\Gamma(1, 2)}{2} \left\{ a_2 \bar{a}_1 F_0^{-1}(a_1) [F_0^{-1}(a_2)]^2 + b_1 \bar{b}_2 F_0^{-1}(\bar{b}_1) [F_0^{-1}(\bar{b}_2)]^2 \right. \\
&\quad - a_2 b_1 F_0^{-1}(\bar{b}_1) [F_0^{-1}(a_2)]^2 - a_1 b_2 F_0^{-1}(a_1) [F_0^{-1}(\bar{b}_2)]^2 \\
&\quad - (1 - a_1 - b_2) \left[a_1 [F_0^{-1}(a_1)]^2 + b_2 [F_0^{-1}(\bar{b}_2)]^2 \right] c_1(a_1, \bar{b}_2) \\
&\quad - (1 - a_1 - b_2) [a_1 F_0^{-1}(a_1) + b_1 F_0^{-1}(\bar{b}_1)] c_2(a_1, \bar{b}_2) \\
&\quad - (1 - a_1 - b_2)^2 c_1(a_1, \bar{b}_2) c_2(a_1, \bar{b}_2) \\
&\quad + (1 - a_1 - b_2) c_3(a_1, \bar{b}_2) \\
&\quad + (1 - a_1 - b_1) \left[a_1 [F_0^{-1}(a_1)]^2 - a_2 [F_0^{-1}(a_2)]^2 \right] c_1(a_1, \bar{b}_1) \\
&\quad + (a_1 - a_2) \left\{ \bar{a}_1 F_0^{-1}(a_1) - b_1 F_0^{-1}(\bar{b}_1) - (1 - a_1 - b_1) c_1(a_1, \bar{b}_1) \right\} c_2(a_2, a_1) \\
&\quad \left. + (b_2 - b_1) \left\{ \bar{b}_2 [F_0^{-1}(\bar{b}_2)]^2 - a_1 [F_0^{-1}(a_1)]^2 - (1 - a_1 - b_2) c_2(a_1, \bar{b}_2) \right\} c_1(\bar{b}_2, \bar{b}_1) \right\}, \\
\Lambda_{221} &= \Lambda_{111}, \text{ with } a_1 \text{ replaced by } a_2 \text{ and } b_1 \text{ replaced by } b_2, \\
\Lambda_{222} &= \Gamma(2, 2) \int_{a_2}^{\bar{b}_2} \int_{a_2}^{\bar{b}_2} K(w, v) F_0^{-1}(w) dF_0^{-1}(v) dF_0^{-1}(w) dv dw \\
&= \frac{\Gamma(2, 2)}{2} \left\{ a_2 \bar{a}_2 [F_0^{-1}(a_2)]^3 + b_2 \bar{b}_2 [F_0^{-1}(\bar{b}_2)]^3 \right. \\
&\quad - a_2 b_2 F_0^{-1}(a_2) F_0^{-1}(\bar{b}_2) [F_0^{-1}(a_2) + F_0^{-1}(\bar{b}_2)] \\
&\quad - (1 - a_2 - b_2) \left[a_2 [F_0^{-1}(a_2)]^2 + b_2 [F_0^{-1}(\bar{b}_2)]^2 \right] c_1(a_2, \bar{b}_2) \\
&\quad - (1 - a_2 - b_2) [a_2 F_0^{-1}(a_2) + b_2 F_0^{-1}(\bar{b}_2)] c_2(a_2, \bar{b}_2) \\
&\quad - [\Gamma(2, 2)]^{-1} c_1(a_2, \bar{b}_2) c_2(a_2, \bar{b}_2) + (1 - a_2 - b_2) c_3(a_2, \bar{b}_2) \left. \right\}, \\
\Lambda_{223} &= \Gamma(2, 2) \int_{a_2}^{\bar{b}_2} \int_{a_2}^{\bar{b}_2} K(w, v) F_0^{-1}(w) F_0^{-1}(v) dF_0^{-1}(v) dF_0^{-1}(w) dv dw \\
&= \frac{\Gamma(2, 2)}{4} \left\{ a_2 \bar{a}_2 [F_0^{-1}(a_2)]^4 + b_2 \bar{b}_2 [F_0^{-1}(\bar{b}_2)]^4 - 2a_2 b_2 [F_0^{-1}(a_2)]^2 [F_0^{-1}(\bar{b}_2)]^2 \right. \\
&\quad - 2(1 - a_2 - b_2) \left[a_2 [F_0^{-1}(a_2)]^2 + b_2 [F_0^{-1}(\bar{b}_2)]^2 \right] c_2(a_2, \bar{b}_2) \\
&\quad - [\Gamma(2, 2)]^{-1} c_2^2(a_2, \bar{b}_2) + (1 - a_2 - b_2) c_4(a_2, \bar{b}_2) \left. \right\}.
\end{aligned}$$

Note 10. The notations Λ_{ijk} , for $1 \leq i, j \leq 2$ and $1 \leq k \leq 3$, can be similarly evaluated under the trimming inequality (15), i.e., (31), as noted in Note 1. \square

It follows that Eq. (48) is equivalent to Eq. (21), and Eq. (50) is equivalent to Eq. (24), under the substitutions $\log(\sigma) \mapsto \theta$, $\beta \mapsto -\sigma$, and $\Delta(u) \mapsto F_0^{-1}(u)$ for $u \in (0, 1)$. Consequently, the expressions for Ψ_{ijk} , with $1 \leq i, j \leq 2$ and $1 \leq k \leq 3$, as defined in Eqs. (63)–(64), can be obtained by applying Theorem 1 under the trimming inequality (25), following the structure of Λ_{ijk} for the same index ranges, and are given below:

$$\Psi_{111} = \Gamma(1, 1) \int_{a_1}^{\bar{b}_1} \int_{a_1}^{\bar{b}_1} \frac{K(w, v)}{vw \log(v) \log(w)} dv dw$$

$$\begin{aligned}
&= \Gamma(1, 1) \left\{ a_1 \bar{a}_1 [\Delta(a_1)]^2 + b_1 \bar{b}_1 [\Delta(\bar{b}_1)]^2 - 2 a_1 b_1 \Delta(a_1) \Delta(\bar{b}_1) \right. \\
&\quad \left. - 2(1 - a_1 - b_1) [a_1 \Delta(a_1) + b_1 \Delta(\bar{b}_1)] \kappa_1(a_1, \bar{b}_1) \right. \\
&\quad \left. - [\Gamma(1, 1)]^{-1} \kappa_1^2(a_1, \bar{b}_1) + (1 - a_1 - b_1) \kappa_2(a_1, \bar{b}_1) \right\}, \\
\Psi_{121} &= \Gamma(1, 2) \int_{a_1}^{\bar{b}_1} \int_{a_2}^{\bar{b}_2} \frac{K(w, v)}{vw \log(v) \log(w)} dv dw \\
&= \Gamma(1, 2) \left\{ a_2 \bar{a}_1 \Delta(a_1) \Delta(a_2) + b_1 \bar{b}_2 \Delta(\bar{b}_1) \Delta(\bar{b}_2) \right. \\
&\quad - a_1 b_2 \Delta(a_1) \Delta(\bar{b}_2) - a_2 b_1 \Delta(a_2) \Delta(\bar{b}_1) \\
&\quad - (1 - a_1 - b_2) [2a_1 \Delta(a_1) + b_1 \Delta(\bar{b}_1) + b_2 \Delta(\bar{b}_2)] \kappa_1(a_1, \bar{b}_2) \\
&\quad - (1 - a_1 - b_2)^2 \kappa_1^2(a_1, \bar{b}_2) + (1 - a_1 - b_2) \kappa_2(a_1, \bar{b}_2) \\
&\quad + (1 - a_1 - b_1) [a_1 \Delta(a_1) - a_2 \Delta(a_2)] \kappa_1(a_1, \bar{b}_1) \\
&\quad + (a_1 - a_2) \left\{ \bar{a}_1 \Delta(a_1) - b_1 \Delta(\bar{b}_1) - (1 - a_1 - b_1) \kappa_1(a_1, \bar{b}_1) \right\} \kappa_1(a_2, a_1) \\
&\quad \left. + (b_2 - b_1) \left\{ \bar{b}_2 \Delta(\bar{b}_2) - a_1 \Delta(a_1) - (1 - a_1 - b_2) \kappa_1(a_1, \bar{b}_2) \right\} \kappa_1(\bar{b}_2, \bar{b}_1) \right\}, \\
\Psi_{122} &= \Gamma(1, 2) \int_{a_1}^{\bar{b}_1} \int_{a_2}^{\bar{b}_2} \frac{K(w, v) \log(-\log(v))}{vw \log(v) \log(w)} dv dw \\
&= \frac{\Gamma(1, 2)}{2} \left\{ a_2 \bar{a}_1 \Delta(a_1) [\Delta(a_2)]^2 + b_1 \bar{b}_2 \Delta(\bar{b}_1) [\Delta(\bar{b}_2)]^2 \right. \\
&\quad - a_2 b_1 \Delta(\bar{b}_1) [\Delta(a_2)]^2 - a_1 b_2 \Delta(a_1) [\Delta(\bar{b}_2)]^2 \\
&\quad - (1 - a_1 - b_2) \left[a_1 [\Delta(a_1)]^2 + b_2 [\Delta(\bar{b}_2)]^2 \right] \kappa_1(a_1, \bar{b}_2) \\
&\quad - (1 - a_1 - b_2) [a_1 \Delta(a_1) + b_1 \Delta(\bar{b}_1)] \kappa_2(a_1, \bar{b}_2) \\
&\quad - (1 - a_1 - b_2)^2 \kappa_1(a_1, \bar{b}_2) \kappa_2(a_1, \bar{b}_2) \\
&\quad + (1 - a_1 - b_2) c_3(a_1, \bar{b}_2) \\
&\quad + (1 - a_1 - b_1) \left[a_1 [\Delta(a_1)]^2 - a_2 [\Delta(a_2)]^2 \right] \kappa_1(a_1, \bar{b}_1) \\
&\quad + (a_1 - a_2) \left\{ \bar{a}_1 \Delta(a_1) - b_1 \Delta(\bar{b}_1) - (1 - a_1 - b_1) \kappa_1(a_1, \bar{b}_1) \right\} \kappa_2(a_2, a_1) \\
&\quad \left. + (b_2 - b_1) \left\{ \bar{b}_2 [\Delta(\bar{b}_2)]^2 - a_1 [\Delta(a_1)]^2 - (1 - a_1 - b_2) \kappa_2(a_1, \bar{b}_2) \right\} \kappa_1(\bar{b}_2, \bar{b}_1) \right\}, \\
\Psi_{221} &= \Psi_{111}, \text{ with } a_1 \text{ replaced by } a_2 \text{ and } b_1 \text{ replaced by } b_2, \\
\Psi_{222} &= \Gamma(2, 2) \int_{a_2}^{\bar{b}_2} \int_{a_2}^{\bar{b}_2} \frac{K(w, v) \log(-\log(v))}{vw \log(v) \log(w)} dv dw \\
&= \frac{\Gamma(2, 2)}{2} \left\{ a_2 \bar{a}_2 [\Delta(a_2)]^3 + b_2 \bar{b}_2 [\Delta(\bar{b}_2)]^3 \right. \\
&\quad - a_2 b_2 \Delta(a_2) \Delta(\bar{b}_2) [\Delta(a_2) + \Delta(\bar{b}_2)] \\
&\quad - (1 - a_2 - b_2) \left[a_2 [\Delta(a_2)]^2 + b_2 [\Delta(\bar{b}_2)]^2 \right] \kappa_1(a_2, \bar{b}_2) \\
&\quad - (1 - a_2 - b_2) [a_2 \Delta(a_2) + b_2 \Delta(\bar{b}_2)] \kappa_2(a_2, \bar{b}_2) \\
&\quad \left. - [\Gamma(2, 2)]^{-1} \kappa_1(a_2, \bar{b}_2) \kappa_2(a_2, \bar{b}_2) + (1 - a_2 - b_2) \kappa_3(a_2, \bar{b}_2) \right\},
\end{aligned}$$

$$\begin{aligned}
\Psi_{223} &= \Gamma(2, 2) \int_{a_2}^{\bar{b}_2} \int_{a_2}^{\bar{b}_2} \frac{K(w, v) \log(-\log(v)) \log(-\log(w))}{vw \log(v) \log(w)} dv dw \\
&= \frac{\Gamma(2, 2)}{4} \left\{ a_2 \bar{a}_2 [\Delta(a_2)]^4 + b_2 \bar{b}_2 [\Delta(\bar{b}_2)]^4 - 2a_2 b_2 [\Delta(a_2)]^2 [\Delta(\bar{b}_2)]^2 \right. \\
&\quad - 2(1 - a_2 - b_2) \left[a_2 [\Delta(a_2)]^2 + b_2 [\Delta(\bar{b}_2)]^2 \right] \kappa_2(a_2, \bar{b}_2) \\
&\quad \left. - [\Gamma(2, 2)]^{-1} \kappa_2^2(a_2, \bar{b}_2) + (1 - a_2 - b_2) \kappa_4(a_2, \bar{b}_2) \right\}.
\end{aligned}$$

Note 11. As discussed in Notes 10 and 1, the notations Ψ_{ijk} , for $1 \leq i, j \leq 2$ and $1 \leq k \leq 3$, can be similarly evaluated under the trimming inequality (15), that is, (31). \square